

1 Morphology of a large paleo-lake: analysis of compaction in the Miocene-
2 Quaternary Pannonian Basin

3

4 Attila Balázs ^{a,b,*}, Imre Magyar ^{c,d}, Liviu Matenco ^a, Orsolya Sztanó ^e, Lilla Tókécs ^e, and
5 Ferenc Horváth ^{b,f}

6

7 ^a Tectonics Group, Department of Earth Sciences, Faculty of Geosciences, Utrecht University,
8 Utrecht, The Netherlands;

9 ^b Department of Geophysics and Space Sciences, Eötvös Loránd University, Budapest,
10 Hungary;

11 ^c MTA-MTM-ELTE Research Group for Paleontology, Budapest, Hungary;

12 ^d MOL Hungarian Oil and Gas Plc, Budapest, Hungary;

13 ^e Department of Physical and Applied Geology, Eötvös Loránd University, Budapest,
14 Hungary;

15 ^f Geomega Ltd., Budapest, Hungary.

16

17

18

19

20 * Corresponding author: Tectonics Group, Department of Earth Sciences, Utrecht University, Budapestlaan 6, 3584 CD
21 Utrecht, The Netherlands; balatt@gmail.com

22

23 **Abstract**

24 Lake-floor morphologies may be significantly different from seafloor topographies of other
25 basins, typically observed in passive or active continental margins. The bathymetry of large
26 paleo-lakes is often overwritten by subsequent tectonic evolution, burial beneath thick
27 overburden and inherent compaction effects. We study the evolution of such an initial
28 underfilled, balance fill and finally overfilled large paleo-lake basin by the interpretation of 2D
29 and 3D seismic data set corroborated with calibrating wells in the example of the Neogene
30 Pannonian Basin of Central Europe. Lake Pannon persisted for about 7-8 Myr and was
31 progressively filled by clastic material sourced by the surrounding mountain chains and
32 transported by large rivers, such as the paleo-Danube and paleo-Tisza. We combined
33 sedimentological observations with a backstripping methodology facilitated by well lithology
34 and porosity data to gradually remove the sediment overburden. This approach has resulted in
35 a morphological reconstruction of the former depositional surfaces with special focus on the
36 prograding shelf-margin slopes. Our calculations show that the water depth of the lake was
37 more than 1000 meters in the deepest sub-basins of the Great Hungarian Plain of the Pannonian
38 Basin. The significant compaction associated with lateral variations of Neogene sediment
39 thicknesses has created non-tectonic normal fault offsets and folds. These features have
40 important effects on fluid migration and hydrocarbon trapping. We furthermore compare the
41 geometries and effects of such non-tectonic features with the activity of larger offset sinistral
42 strike-slip zones using 3D seismic attributes.

43 *Keywords:* Lake Pannon, bathymetry, compaction, Pannonian Basin, shelf-margin

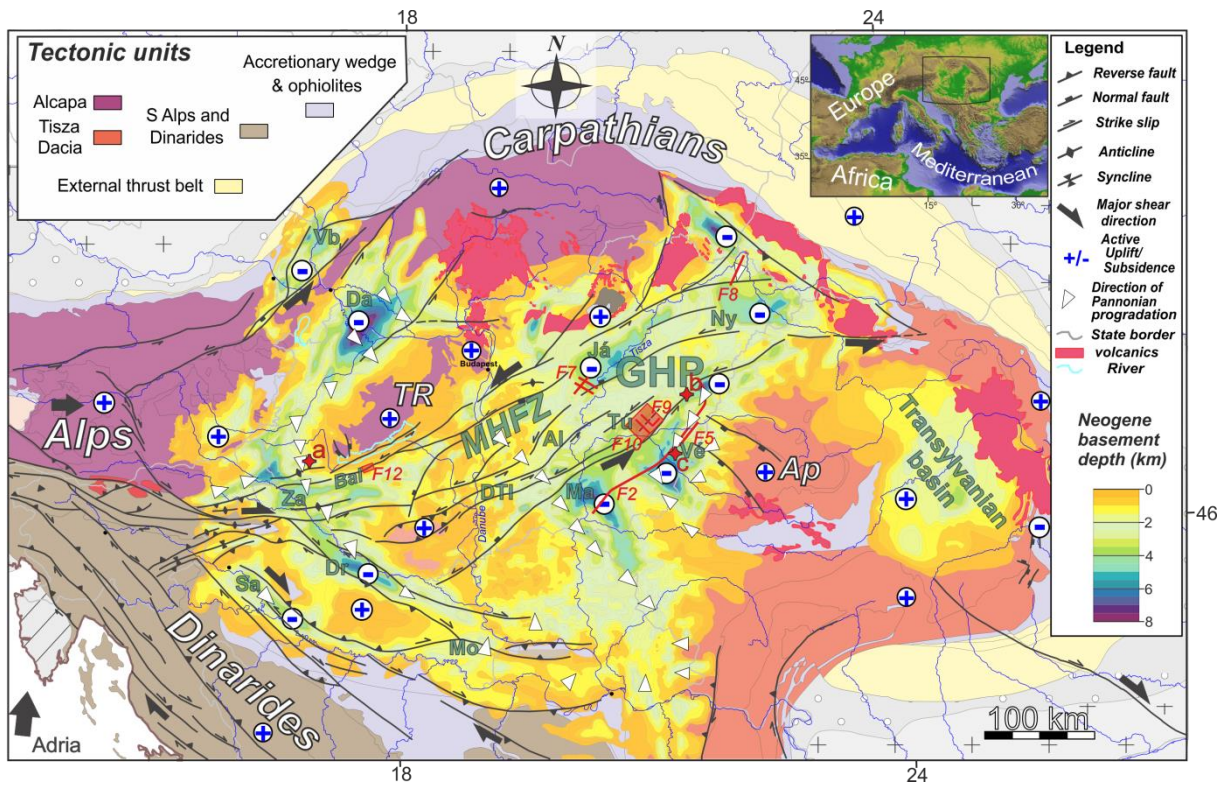
44

45 **1. Introduction**

46 Deep lake basins formed in intra-continental settings affected by large amounts of
47 extension can record the deposition of kilometres thick sediments (Katz, 1990). Paleo-water
48 depth and the sedimentary architecture are controlled by several external forcing factors; their
49 effects and interactions show marked differences from open marine environments (Martins-
50 Neto and Catuneanu, 2010; Sztanó et al., 2013). Lakes are more sensitive to regional climate
51 by the primary control of the local balance between precipitation and evapotranspiration (e.g.,
52 Carroll and Bohacs, 1999). In contrast to passive margins, the subsidence and/or uplift rates in
53 intra-continental settings are also more variable (Xie and Heller, 2009). Lakes are sensitive to
54 episodic (dis)connections with other neighbouring basins through the separating gateways,
55 which are controlled by tectonics and lake level variations (e.g. Leever et al., 2011; ter Borgh
56 et al., 2013; Matenco et al., 2016). This overall interplay between tectonics, lake level
57 variations, sedimentation rates and transport routing results in spatially and temporally
58 heterogeneous depositional environments (Garcia-Castellanos et al., 2003; de Leeuw et al.,
59 2012; ter Borgh et al., 2015).

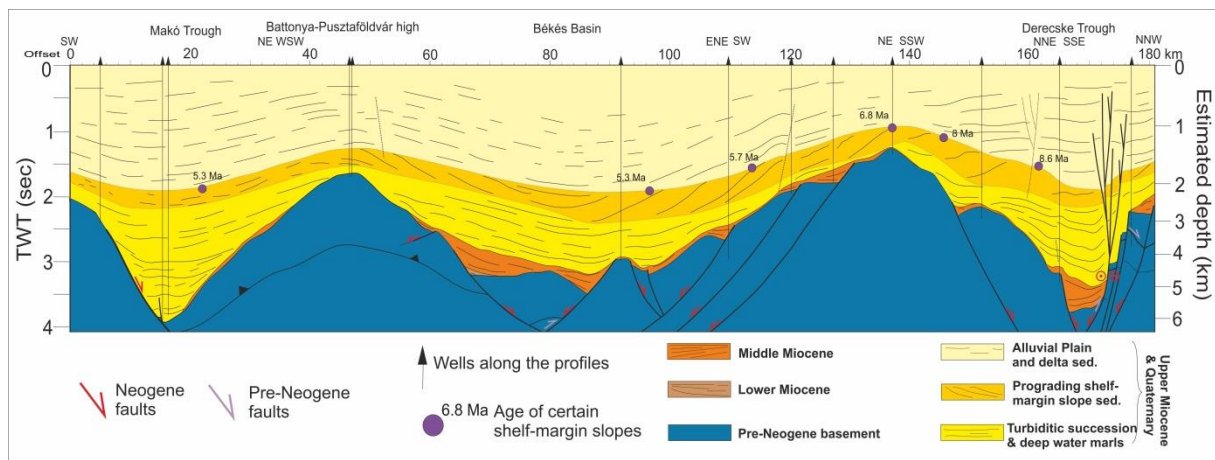
60 A typical example where a high-resolution data set is available for the analysis of the
61 formation and evolution of a paleo-lake is the Pannonian Basin of Central Europe (Fig. 1). The
62 paleo-Danube and paleo-Tisza rivers discharged large volumes of sediments into Lake Pannon
63 during Late Miocene - Early Pliocene times in a sink area that roughly comprised the Vienna,
64 Pannonian and Transylvanian basins. The lake persisted for 7-8 Myrs and was progressively
65 filled by, and buried under, clastic material sourced by the surrounding mountain chains (e.g.,
66 Magyar et al. 2013). The long-standing hydrocarbon exploration activity of the basin has
67 resulted in the availability of high-resolution geophysical data including well logs and 2D/3D
68 seismic data (e.g., Bérczi and Phillips, 1985; Royden and Horváth, 1988; Pogácsás et al., 1988;
69 Juhász, 1991; Grow et al., 1994; Vakarcs et al., 1994; Saftic et al., 2003; Magyar et al., 2006;

70 Sztanó et al., 2013) that allow a high prospectivity for conventional and unconventional geo-
 71 resources including geothermal energy (e.g., Cloetingh et al., 2010; Horváth et al., 2015).
 72 Lacustrine organic-rich shales define good hydrocarbon source rocks, while deep-water
 73 turbidites, deltaic and fluvial sand bodies are important reservoirs (Saftić et al., 2003; Magyar
 74 et al., 2006; Tari and Horváth, 2006).



75
 76 **Figure 1.** Tectonic map of the Pannonian Basin and adjacent areas showing the neotectonic
 77 fault pattern and active differential vertical movements (modified after Bada et al., 2007)
 78 overlain by the depth of the pre-Neogene basement. The tectonic units of the pre-Tertiary
 79 basement outcropping on the flanks of the basin are simplified after Schmid et al. (2008). GHP
 80 – Great Hungarian Plain, Vb – Vienna basin, MHFZ – Mid-Hungarian Fault Zone, Bal –
 81 Balaton Fault zone, TR – Transdanubian Range, Ny – Nyírség sub-basin, Já – Jászság sub-
 82 basin, Al – Alpár sub-basin, Ma – Makó Trough, Vé – Vésztó Trough, Tú – Túrkeve Trough,
 83 DTI – Danube-Tisza interfluvium, Da – Danube basin, Za – Zala sub-basin, Dr – Drava Trough,

84 Sa – Sava Trough, Mo – Morovic depression, Ap – Apuseni Mountains. Well locations of
85 Figure 4 (a,b,c) are marked by red cross symbols.



87 **Figure 2.** Interpreted composite seismic section from the eastern part of the Great Hungarian
88 Plain (modified after Balázs et al., 2016). For location see Fig. 1. Note the long wavelength
89 folding of the young sediments partly caused by compaction effects.

90 In order to understand the morphology of depositional surfaces and evolution of such a
91 deeply buried lacustrine system, we have performed 2D and 3D seismic interpretation and
92 backstripping in the up to ~7 km thick Pannonian Neogene sediments (Fig. 2). Paleo-
93 bathymetric estimates were derived by successive decompaction of prograding shelf-margin
94 slope clinoforms based on the available lithology and porosity data from wells in different
95 regions of the Pannonian Basin. We have analysed the spatial and temporal variation of
96 clinoform geometries and shelf-edge trajectories (e.g., Helland-Hansen and Hampson, 2009;
97 Henriksen et al., 2011; Rabineau et al., 2014) controlled by the interplay between high sediment
98 fluxes, inherited pre-Neogene basement geometries, paleo-water depth, the rate of subsidence
99 interrupted by periods of tectonically-induced uplift and climatically controlled lake level
100 variations. We have furthermore analysed the effects of the few kilometres thick overburden
101 and the variable relief of the basin floor in creating significant compaction effects, such as long
102 wavelength folds and differential compaction induced faults (e.g., Magara, 1978; Williams,
103 1987; Xu et al., 2015).

104

2. Evolution of the Pannonian Basin and Lake Pannon

105

The Pannonian basin of Central Europe is a Neogene continental back-arc basin, where

106

the 220-290 km of Miocene extension is accommodated by the roll-back of the Carpathians and

107

Dinaridic slabs (Fig. 1, Ustaszewski et al., 2010; Matenco and Radivojevic, 2012; Faccenna et

108

al., 2014; Horváth et al., 2015 and references therein). Extensional basin formation followed a

109

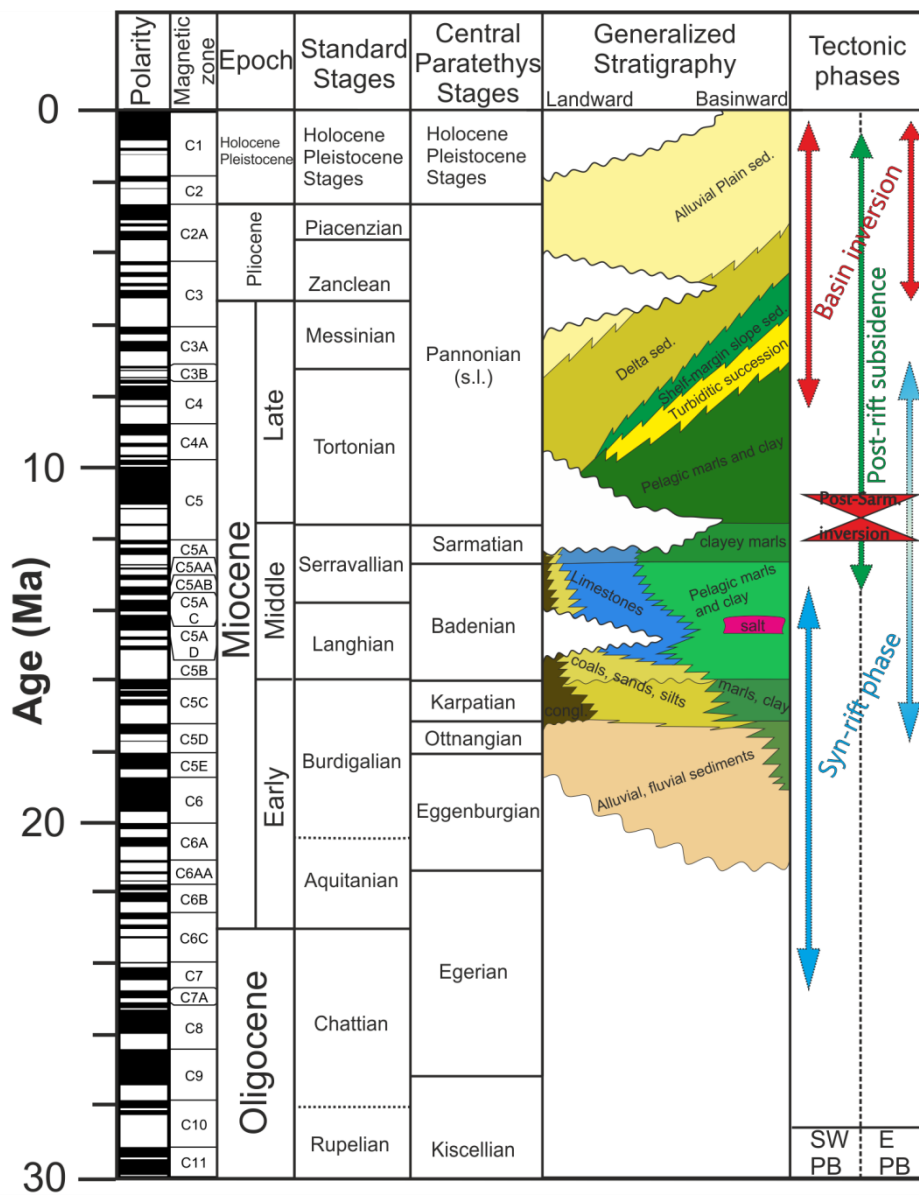
pre-Neogene orogenic evolution that resulted from the opening and subsequent closure of two

110

oceanic realms, the Triassic-Cretaceous Neotethys and Middle Jurassic – Paleogene Alpine

111

Tethys (e.g., Schmid et al., 2008 and references therein).



112

113 **Figure 3.** Tectono-stratigraphic chart of the Great Hungarian Plain part of the Pannonian Basin
114 with correlation of the standard and Central Paratethys stages, the generalized Miocene
115 lithostratigraphy of the study area and the main tectonic phases affecting the basin (modified
116 after Balázs et al., 2016). Note that the syn-rift/post-rift boundary and the onset of the latest
117 stage basin inversion are older in the SW and progressively younger E-NE -wards.

118 Starting from the late Eocene times the uplift of the Alpine – Himalayan mountain belt
119 has gradually fragmented the larger Tethys Ocean and formed the Paratethys branch. The area
120 of the future Pannonian Basin became part of the Central Paratethys, a semi-enclosed marine
121 to lacustrine basin system (Báldi, 1989; Nagymarosy and Müller, 1988; Rögl and Daxner-Höck,
122 1996). Lower Miocene sediments were deposited in fluvial, lacustrine and locally marine
123 conditions (Báldi, 1986; Nagymarosy and Hámor, 2012). The Middle Miocene is the time when
124 the subsidence associated with extension resulted in the deposition of deep basinal sediments
125 in the centre of extensional (half) grabens, while deposition along their margins was dominated
126 by near-shore to shallow-marine conditions (Kováč et al., 2007; Nagymarosy and Hámor,
127 2012). The uplift of the Carpathians and Dinarides (ter Borgh et al., 2013) and further mantle
128 dynamics (see Balázs et al., 2016) led to the formation of an unconformity between the Middle
129 and Upper Miocene strata marking the disruption of connections with the Paratethys Sea and
130 development of the large, brackish, isolated Lake Pannon (Fig. 3; Magyar et al., 1999). An up
131 to 7 km thick sedimentary succession was deposited during Late Miocene to recent times in the
132 Great Hungarian Plain, the area with recording most of the stretching in the Pannonian Basin
133 (Figs. 1, 2, Horváth et al., 2015). The basin fill recorded an initial transgression resulting in a
134 period of underfilled stage. It was followed by shelf margin and slope progradation fed by the
135 influx of sediments via fluvial systems resembling the present-day Danube and Tisza rivers.
136 The largest spatial extension of Lake Pannon was at ~9.5 Ma (Magyar et al., 1999), covering
137 the Vienna, Pannonian and Transylvanian basins. The shelf-margin prograded about 500 km in

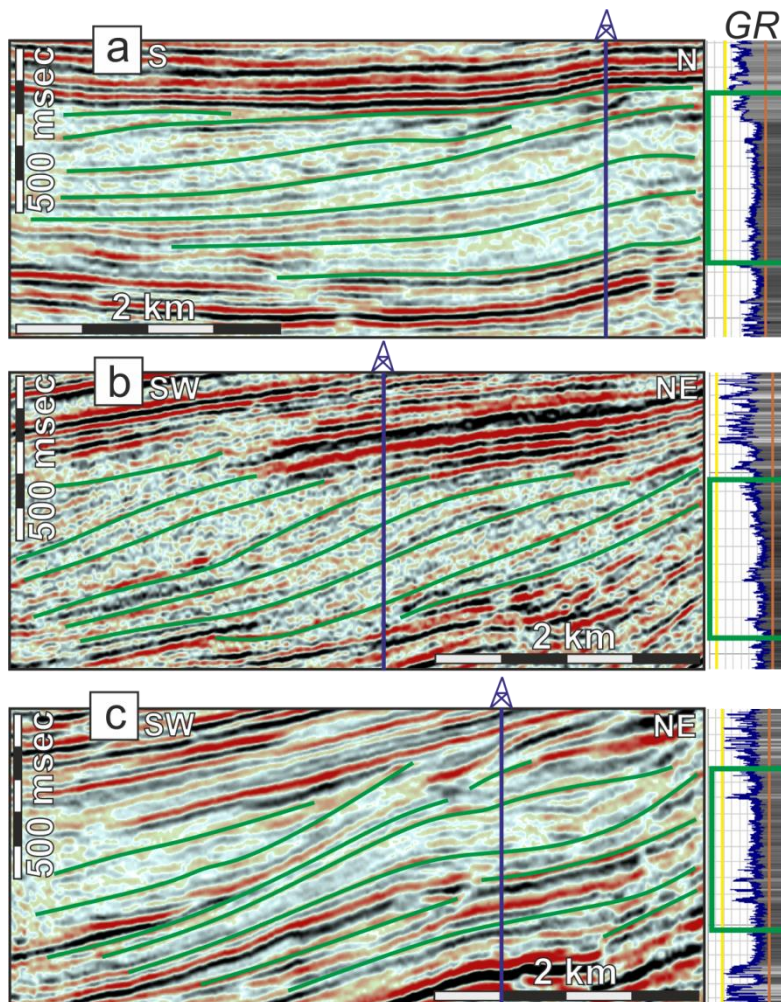
138 6 Myrs until the early Pliocene from the NW and NE in a ~S-SE direction, while minor
139 progradation was recorded from other directions (Pogácsás et al., 1988; Vakarcs et al., 1994;
140 Magyar et al., 2013; ter Borgh et al., 2015). The coeval sedimentation reflects the deposition of
141 several diachronous lithostratigraphic formations (Fig. 2) that were deposited in response to the
142 progradation from deep to shallow lake environments (Fig. 3, Bérczi and Phillips, 1985; Juhász,
143 1991; Sztanó et al., 2013). These associations are laterally variable from deep hemi-pelagic
144 deposition (Endrőd Formation), turbidites (Szolnok Formation), shelf-margin slope (Algyő
145 Formation) and delta (Újfalu Formation) to alluvial plain sediments (Zagyva Formation). Their
146 typical seismic expression provides an excellent lateral correlativity of seismic facies units.

147 Extension and subsequent thermal subsidence in the Pannonian Basin was followed by
148 a period of basin inversion that started at ~8 Ma (Uhrin et al., 2009), observed by accelerated
149 differential vertical movements and fault reactivations (Horváth and Cloetingh, 1996; Fodor et
150 al., 2005; Bada et al., 2007; Dombrádi et al., 2010). Active sinistral faults with ENE-WSW
151 strike are interpreted in the centre of the basin and dextral shear zones with WNW-ESE strike
152 at its southern margin (Fig. 1, Horváth et al., 2006). Several unconformities are observed during
153 these times in the basin fill (e.g., Vakarcs et al., 1994). One unconformity is dated at ~6.8 Ma.
154 Another unconformity is observed near the boundary between the Miocene and Pliocene (e.g.,
155 Vakarcs et al., 1994), being angular and locally erosional near the basin margins and passes to
156 a correlative conformity towards the basin centre. These unconformities are variably interpreted
157 as either related to basin inversion (Sacchi et al., 1999; Magyar and Sztanó, 2008; ter Borgh et
158 al., 2015), or formed in response to major lake level variations (Csató et al., 2015), or
159 representing cross-over zones of different progradational directions reflected by onlap patterns
160 in slope deposits (Magyar and Sztanó, 2008).

161

162 **3. Data and methods**

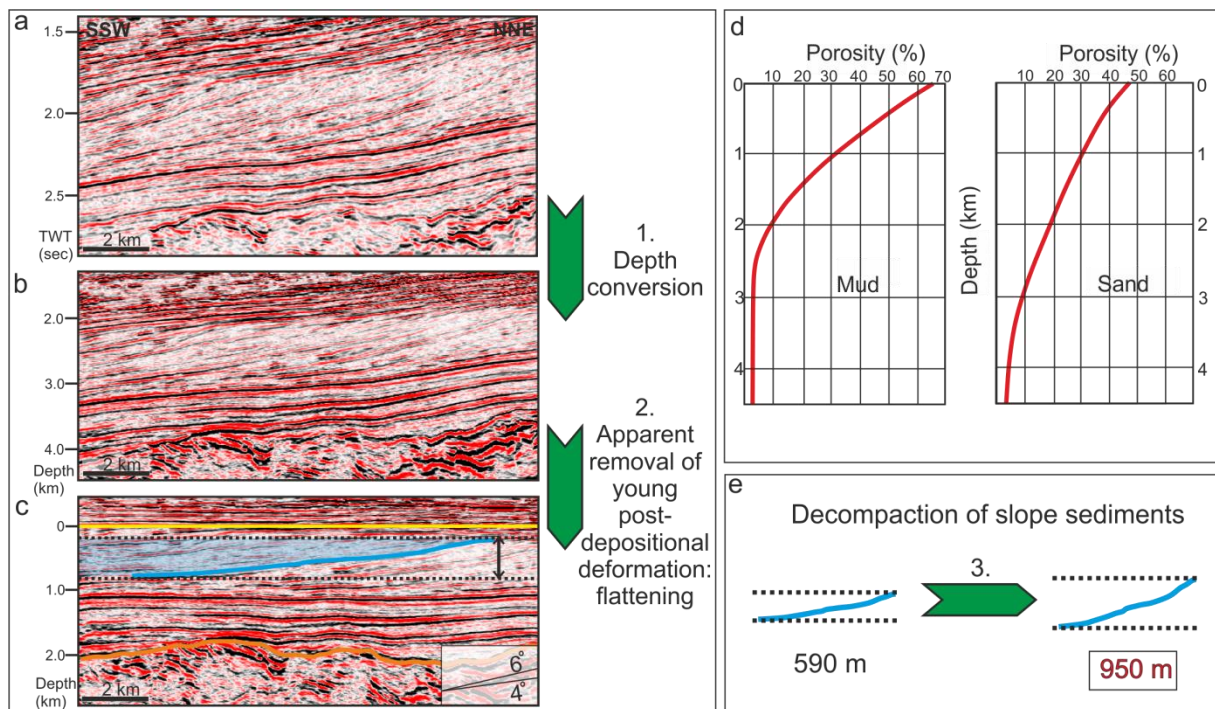
163 We have analysed a large array of 2D and 3D seismic data calibrated by a dense network
164 of exploration wells. This analysis is illustrated by the selection of several key seismic lines
165 and wells, generally oriented parallel with the direction of sediment transport (e.g., Fig. 4). The
166 signal/noise ratio and resolution of the seismic sections are variable, and reflect the availability
167 of data, from recent 3D seismic surveys to older 2D seismic lines. The vertical resolution
168 averages 20-30 meters at the depth of 2-3 kilometres. Well-logs were tied to seismic sections
169 using standard VSPs and check-shots, the error-bar is generally below the seismic resolution
170 (see also Mészáros and Zilahi-Sebess, 2001).



171
172 **Figure 4.** Seismic sections parallel with the direction of progradation and gamma ray logs
173 showing the characteristic seismic facies and lithology of the prograding shelf-margin slope
174 sediments. Slope clinoforms are indicated by green lines, green box indicates the interval of

175 slope sediments on well logs. Note the low-amplitude seismic facies, fine grained lithology of
 176 the unit and the gentle tilting post-dating the deposition of the slope sediments. Well locations
 177 (a-c) are displayed in Figure 1.

178 Our interpretation is focused on the prograding shelf-margin slope clinoforms
 179 connecting the shelf with the deep part of the basin. The slope sediments are associated with a
 180 medium to low amplitude, continuous-discontinuous alternating, high frequency seismic facies
 181 grouped in overall clinoform geometry (Figs. 4, 5 and 6, see also Magyar et al., 2013). In
 182 seismic lines oriented perpendicular to the direction of progradation (Fig. 7e) the seismic facies
 183 of the slope sediments is rather hummocky to chaotic. They often show incisions or canyons of
 184 variable magnitudes near the shelf or along the slope as well as turbidite channels and turbidite
 185 channel-levee complexes at the base of slope (see also Juhász et al., 2013; Sztanó et al., 2013).



186
 187 **Figure 5.** Methodology used for paleobathymetrical calculations. The TWT version of the
 188 seismic line (a) is converted to depth (b) and subsequently flattened (c) by using a horizon
 189 located immediately above the prograding clinoform sequence (in the overlying delta deposits,

190 indicated as 0 m depth). (d) We use a lithology dependent porosity-depth function available for
191 these sediments in the Pannonian Basin (after Szalay, 1982) to decompact sediments and
192 calculate the height of shelf-margin slope (e). The distance between topset and bottomset is 590
193 m and 950 m before and after decompaction, respectively.

194 We have performed first a sedimentological and seismo-stratigraphic interpretation by
195 detecting reflection terminations and separating seismic facies units (e.g., Posamentier and
196 Walker, 2006) It was followed by calculating a number of seismic attributes in 3D seismics that
197 allowed a better differentiation of faults and sedimentary features (e.g., Cartwright and Huuse,
198 2005; Chopra and Marfurt, 2005). These attributes are particularly suitable to highlight paleo-
199 geomorphological and structural features. We have used seismic amplitude values extracted on
200 mapped horizons to highlight amplitude anomalies related to sharp acoustic impedance
201 contrasts connected, for instance, with sharp lithological changes. We have also used spectral
202 decomposition (e.g., Partyka et al., 1999) to produce amplitude and phase spectra for targeted
203 windows over horizons. Different discrete frequency values were RGB colour blended and
204 displayed on the interpreted horizon. We have calculated coherency attribute cubes based on
205 the cross-correlation of seismic traces in selected windows to highlight structural features.

206 The bottom morphology of Lake Pannon was derived in a gradual procedure (Fig. 5).
207 Seismic lines were converted to depth (Fig. 5a, b). On top of the lacustrine strata, the upper part
208 of the basin fill is composed by delta and alluvial sediments deposited over a low and flat
209 morphological relief (Sztanó et al., 2007). These sediments show deformation generally
210 characterized by large open folds locally affected by faults with small vertical offsets. The areas
211 affected by local faulting were generally avoided for lake morphology calculations. The effects
212 of the gentle folding were restored by flattening the seismic lines to the first continuous reflector
213 representing the paleo-horizon in the delta and alluvial sediments that is laterally continuous
214 above the clinoforms along the seismic line. The distribution of these sediments (Újfalu and

215 Zagyva Formations) in seismic lines is very well controlled by available wells, where these
216 have characteristic well-log expressions (Fig. 4, Bérczi and Phillips, 1985; Juhász, 1991). In
217 seismic lines the first deposition of the delta deposits is observed as coherent high amplitude,
218 low frequency continuous reflections facies overlying the topsets and clinoforms of the
219 lacustrine progradation (Fig. 5). Given the resolution of the seismic lines, this type of restoration
220 is a very good approximation of the morphology of Lake Pannon, affected by the subsequent
221 compaction.

222 The seismo-stratigraphic interpretation has separated seismic facies units and seismic
223 facies associations (e.g., Fig. 7) in the prograding clinoforms, which were converted into
224 lithological facies units based on available well-logs (mostly gamma-rays, e.g., Fig. 4). The
225 shelf-margin slope foresets are built up by about 80% mudstone combined with 20% sandstone
226 (see also Szalay and Szentgyörgyi, 1988), only the upper and lowermost parts contain higher
227 amounts of sand. Decompaction of the progradation geometry to derive the original
228 morphology of Lake Pannon was achieved by a standard modelling technique (e.g., Angevine
229 et al., 1990) based on the lithology dependent porosity-depth data available for the Great
230 Hungarian Plain (Szalay, 1982; Dövényi, 1994). This 1D modelling was performed in
231 successive places in the basin (Table 1). Note that the first continuous reflector of the delta and
232 alluvial seismic facies may be at different depth across one section, due to the
233 progradation/aggradation geometries. In places where a smaller scale delta progradation was
234 detected in the shelf facies, the flattening was performed at the first continuous reflector
235 overlying this secondary progradation. By connecting successive 1D decompacted geometries,
236 the evolution of the lake morphology was reconstructed along each studied seismic line. This
237 lake morphology gives a minimum estimation of the water depth. These calculations have a
238 resolution close to the seismic one in the proximity of the lake shelf-margin slope, while at
239 farther distances these estimates are less precise (Steckler et al., 1999). Based on existing

240 sedimentological interpretations (Juhász, 1991; Sztanó et al., 2013), an additional 0-75 m water-
241 depth characterized the shelf of the lake (where part of the deltaic sedimentation is located),
242 while at farther distances from the progradation our calculation are just minimum estimates, the
243 paleo-bathymetry could have been much deeper. It is likely that the overall paleo-bathymetry
244 decreases with the approaching progradation by the distal infill of deep-water turbidites and
245 more pelagic sedimentation.

246

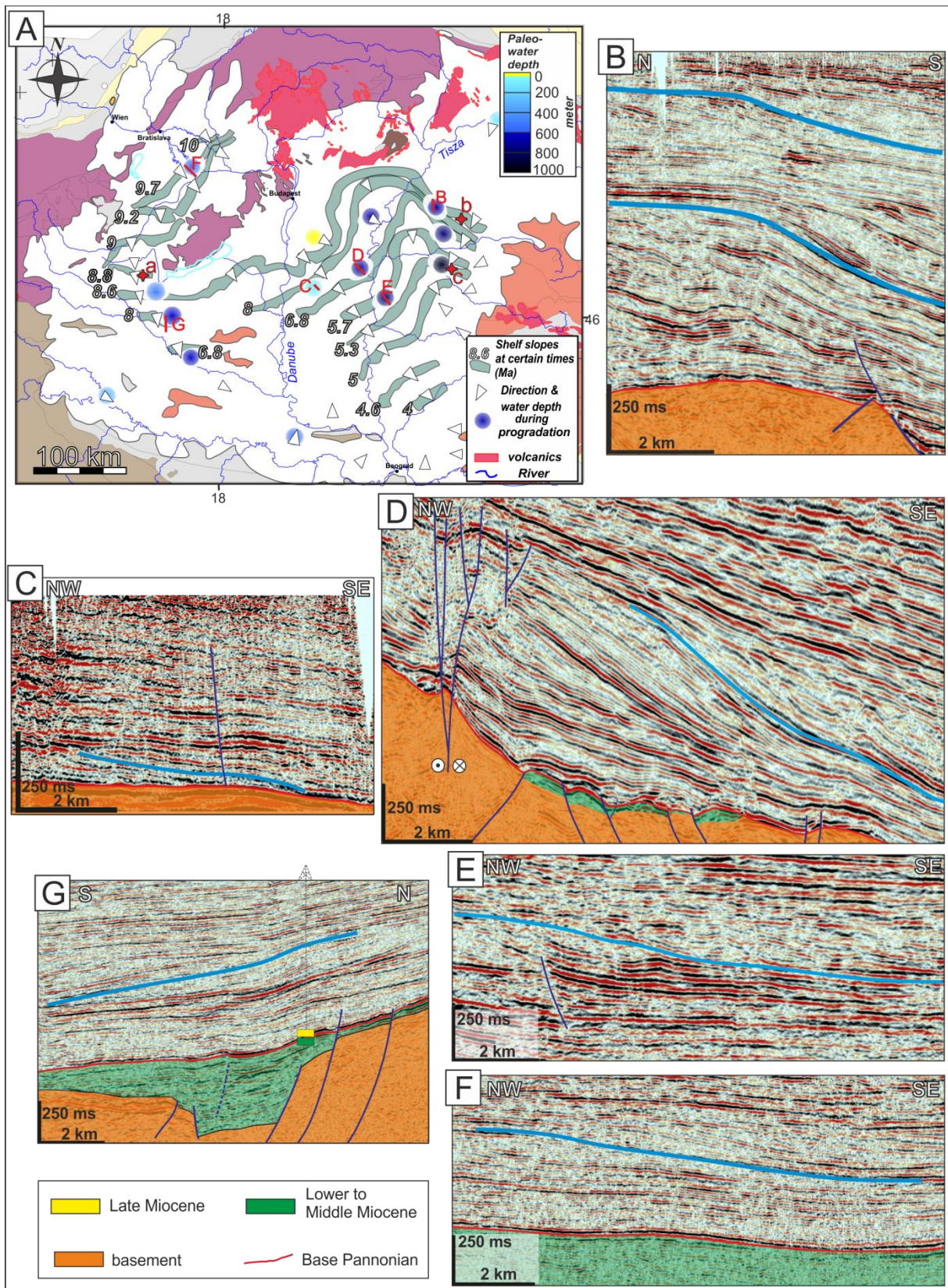
247 **4. Paleobathymetry of Lake Pannon**

248 The general extensional geometry of the Pannonian Basin is characterized by individual
249 sub-basins filled by 1 - 3.5 km of Lower to Upper Miocene syn-kinematic deposits, overlain by
250 a 1.5 - 3.5 km thick post-extensional sedimentary cover. Here we focus on the prograding shelf-
251 margin slope clinoforms that post-date the syn-extensional sedimentation to derive the
252 paleobathymetry of the Late Miocene to Pliocene Lake Pannon.

253 **4.1 Paleobathymetric calculations**

254 Based on the flattened height of the Upper Miocene to Pliocene prograding shelf-margin
255 slope clinoforms, paleobathymetric estimations by decompaction have been carried out in 8
256 representative sub-basins (Fig. 6, Table 1). Seismic section from the Nádudvar sub-basin of the
257 central Great Hungarian Plain (Fig. 6b) shows the initial distribution of Pannonian sediments
258 by prograding shelf-margin slope and delta sediments over deep-water marls and turbidites.
259 This was followed by a base level rise at ~7.5 Ma (Juhász et al., 2007) associated with a major
260 retrogradation and renewed deposition of deep-water sediments over the deltaic succession,
261 overlain by renewed progradation and filling of the basin by deltaic and alluvial sediments in
262 the upper part of the section (Fig. 6b). The calculated evolution of the lake morphology

263 indicates 650 meters for the older clinoforms, up to few tens of metres for the deltaic
 264 environment and 200 meters of paleo-bathymetry for the upper, younger clinoforms.



265

266 **Figure 6.** a) Positions of consecutive prograding shelf-margin slopes during the Miocene –
267 Pliocene sedimentation (modified after Magyar et al., 2013). Blue circles indicate our calculated
268 water depth values, different colours correspond to the paleo-water depth scale. Red cross
269 symbols with small letters (a-c) show the well positions of Figure 4. B-F are the locations of
270 the seismic sections in this figure showing the shelf-margin slopes used for paleobathymetric
271 estimations; b) Seismic line in the Nádudvar sub-basin; c) Seismic section in the Danube-Tisza
272 interfluve; d) Seismic section in the Alpár sub-basin; e) Seismic section in the Makó Trough;
273 f) Seismic section in the Danube Basin; g) Seismic section in the Zala Basin.

Location	Age (Ma)	Section	Compacted height (m)	Decompacted height (m)
Jászság sub-basin	~ 7 Ma	Figure 7	440	690
Jászság sub-basin	~ 7 Ma	Figure 7	450	690
Jászság sub-basin	~ 7 Ma	Figure 7	370	580
Túrkeve sub-basin	~ 5.7 Ma	Figure 9, location a)	290	510
Túrkeve sub-basin	~ 5.7 Ma	Figure 9, location b)	350	630
Túrkeve sub-basin	~ 5.7 Ma	Figure 9, location c)	255	470
Túrkeve sub-basin	~ 5.7 Ma	Figure 9, location d)	455	740
N Nyírség sub-basin	~ 10 Ma	Figure 8, delta, location 1	48	70
N Nyírség sub-basin	~ 10 Ma	Figure 8, slope, location 2	91	150
Makó Trough	~ 5.7 Ma	Figure 6e	425	750
Nádudvar sub-basin	~ 7.5 Ma	Figure 6b upper blue line	180	200
Nádudvar sub-basin	~ 8.6 Ma	Figure 6b lower blue line	400	650
Danube Basin	~ 10 Ma	Figure 6f	280	550
Zala Basin	~ 8 Ma	Figure 6g	340	600
Alpár sub-basin	~ 7 Ma	Figure 6d	420	675
Danube-Tisza interfluve	~ 7.5 Ma	Figure 6c	75	130
Vésztő Trough	~ 5.3 Ma	Figure 5	590	950
Sava Trough	~ 6.5? Ma	*	185	275
Morovic depression	~ 4.5? Ma	*	350	525

274 **Table 1.** Height of the clinoforms before and after decompaction, the latter represents a
275 minimum estimation of the paleo-water depth. *Seismic data used for our paleobathymetric
276 estimation for the Sava Trough and Morovic depression are from Ustaszewski et al. (2014) and
277 ter Borgh et al. (2015), respectively.

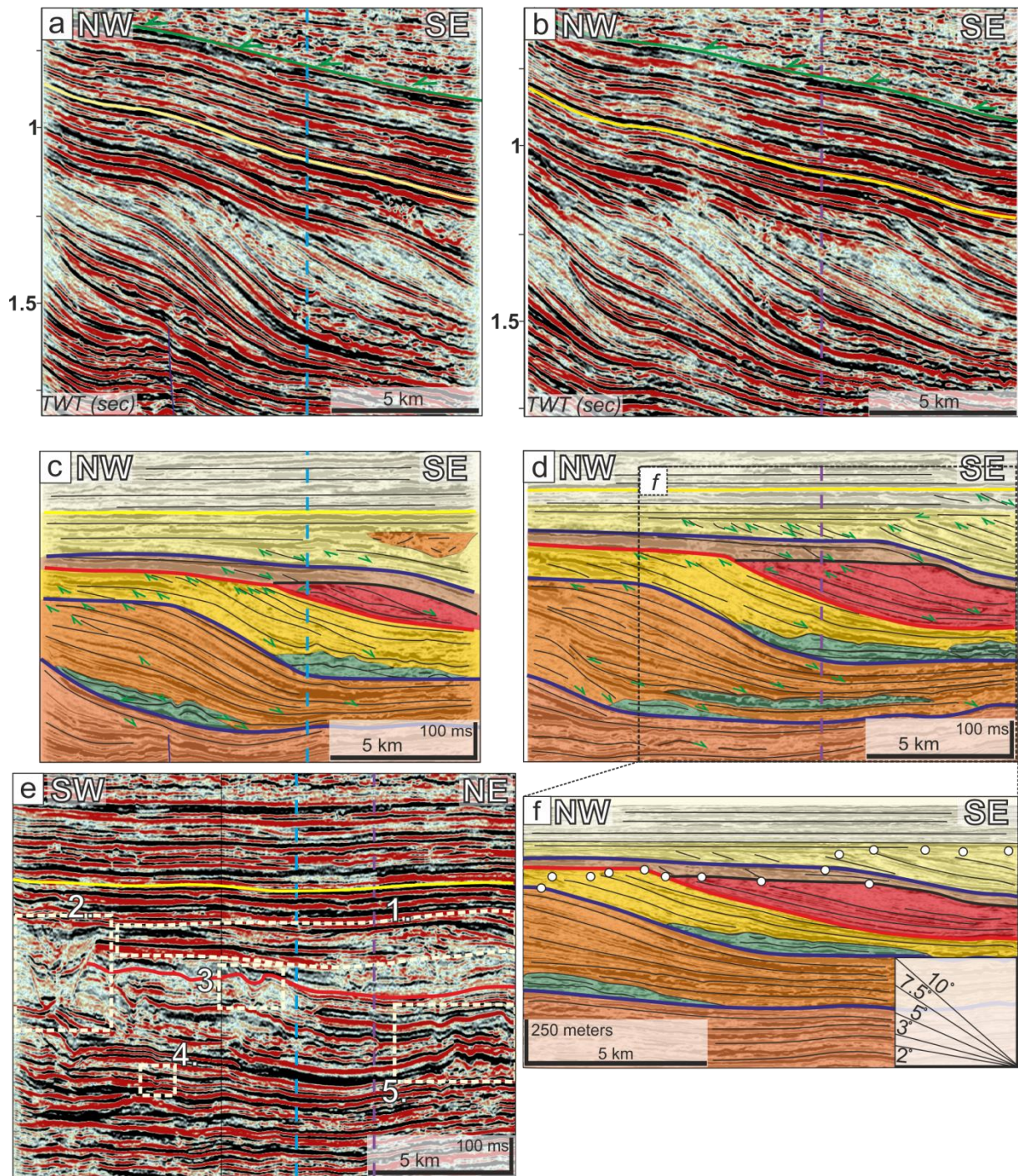
278

279 Seismic section from the central part of the Great Hungarian Plain between the present-day
280 Danube and Tisza rivers (Figs. 1 and 6c) shows a thin prograding sequence with decompacted
281 paleo-bathymetries of ~130 m that is laterally slightly higher in the area above the Middle
282 Miocene (half) grabens. To the northeast, seismic sections form the Alpár sub-basin (Fig. 6d)
283 show an inverted basement high to the NW, while the depth of this basement increases SE-
284 wards. The calculated paleo-water depth is ~675 meters, the age of progradation in this area
285 being 7-6.8 Ma (Magyar et al., 2013). We note that multiple phases of inversion and strike-slip
286 deformation observed in the sediments overlying the Alpár sub-basin have also created a large
287 incised canyon system at ca. 6.8 Ma (Juhász et al., 2013). Subsequently it was followed from
288 ~5.3 Ma by continuous differential vertical movements creating the tilting observed in our
289 seismic line (Fig. 6d). To the southeast, the ~5.7 Ma progradation observed in the Makó Trough
290 (Sztanó et al., 2013) has ~750 m calculated paleobathymetries (Fig. 1, 6e), in the centre of this
291 very deep sub-basin, decreasing to 650 m over its flanks (Balázs et al. 2015). In the western
292 part of Lake Pannon, the SE-ward progradation of the paleo-Danube took place between 10-6.8
293 Ma (Magyar et al., 2013). The calculated paleo-bathymetries for this area are 550 m for the NW
294 in the Danube basin (Figs. 1, 6f), 550 m for the Zala (Fig. 6g) and ~600 m for the Drava sub-
295 basins (see also Balázs et al., 2015). These values are in agreement with earlier predictions in
296 this area (Uhrin et al., 2009). In the southern part of the Pannonian Basin, paleo-bathymetric
297 calculations in the Sava Trough and Morovic Depression (Fig. 1, seismic lines in Ustaszewski
298 et al., 2014 and ter Borgh et al., 2015, respectively), indicating E-wards prograding clinoforms
299 paleobathymetries of 275 m and N-ward prograding clinoforms paleobathymetries of 525 m,
300 respectively.

301

302 4.2 The paleo-morphology of Lake Pannon

303 An appropriate place where the fine interplay between the creation of accommodation and
304 sedimentation can be observed is the Jászság sub-basin of the northern part of the Great
305 Hungarian Plain (Fig. 1). This sub-basin was filled by sediments transported by both the paleo-
306 Danube from WNW and the paleo-Tisza from NE directions between ~8-6.8 Ma (Magyar et
307 al., 2013). Two seismic lines (Figs. 7a,b) parallel with the local direction of progradation show
308 the geometries of the shelf-margin slope, delta progradation on the shelf and toe of slope
309 sediment complexes. An angular unconformity between the Miocene and Pliocene sediments
310 (green line in Figs. 7a,b) marks the boundary of delta and alluvial environments as well. Shelf-
311 edge trajectories (Fig. 7f) infer interplay between normal regression, forced regression
312 (reflecting base-level drop of ~80 m), transgression and retrogradation (reflecting a base-level
313 rise of ~200 m). Seismic lines perpendicular to the direction of progradation show that shelf
314 incisions took place during both relative water-level rise and water-level fall (Fig. 7e). This
315 means that such observed incisions or canyons are not necessarily subaerial. They can be also
316 the result of slope failure during rapid transgression (cf., Fongngern et al., 2016).



317

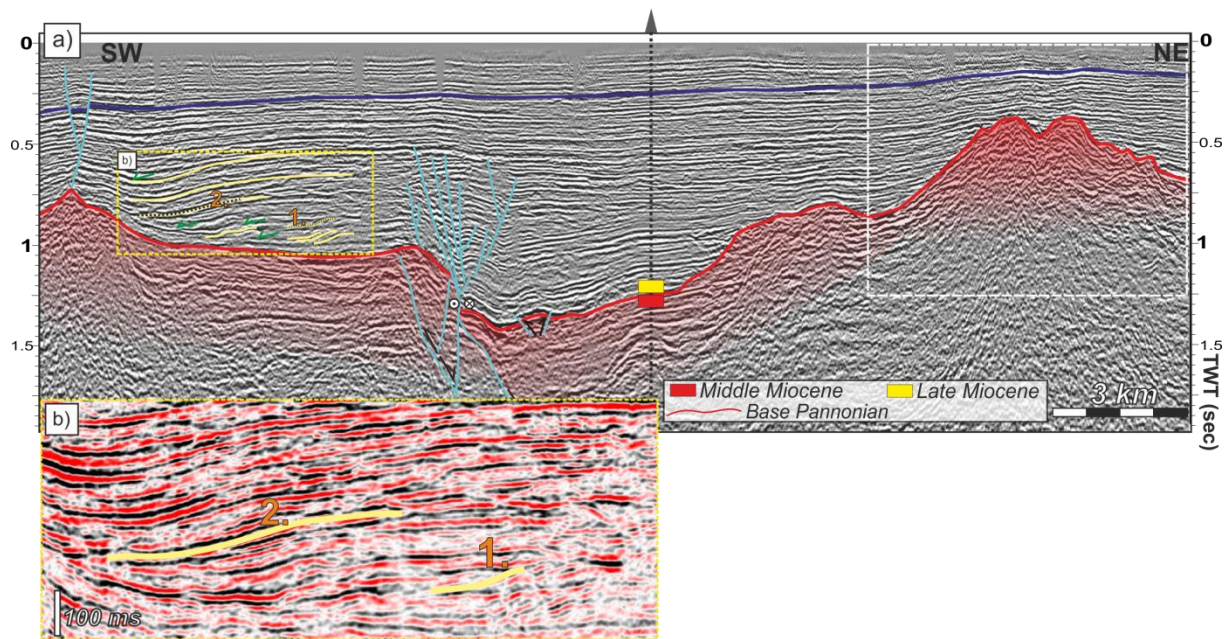
318 **Figure 7.** Seismic sections a) and b) oriented parallel with the direction of progradation in the
 319 Jászág sub-basin. Interpretation (c, d) shows typical progradational (in orange), aggradational
 320 (in yellow), forced regression (red), and retrogradational patterns in the Great Hungarian Plain
 321 (location in Figure 1). Note the turbidite complexes at the toe of slopes (in green). Green half-
 322 arrows are reflection terminations. Green line is the unconformity between Miocene and

323 Pliocene sediments, yellow line is the flattening level; c) and d) are the flattened version of the
324 seismic lines above; e) seismic section in the same area perpendicular to the direction of
325 progradation. Vertical dashed lines are intersections with profiles displayed in Figures 7a and
326 7b. This seismic line shows (1) delta progradation over the shelf area; (2,3) large-scale incisions
327 (~ up to 200 meters deep) near the transition between the shelf and the slope; (4) small turbidite
328 channel within deep water sediments; (5) stacked channel-levee systems (~30-60 m thick); see
329 also Sztanó et al.(2013) and Juhász et al. (2013); f) depth converted version of part of the
330 seismic line in Fig. 7d. Small circles denote the evolution of the shelf margin (i.e., shelf edge
331 trajectories).

332

333 4.3 Effects of inherited extensional half-grabens on the paleobathymetry of 334 Lake Pannon

335 The analysis of the syn-kinematic sedimentation in the diachronous extensional half-
336 grabens is available in previous studies (e.g., Matenco and Radivojevic, 2012, ter Borgh et al.,
337 2015; Balázs et al., 2016). Here we only illustrate the structural history characterizing the
338 evolution of the Pannonian Basin by choosing two specific zones as examples: the Nyírség sub-
339 basin in the north-eastern margin of the Great Hungarian Plain and the Túrkeve sub-basin from
340 the deep central part.

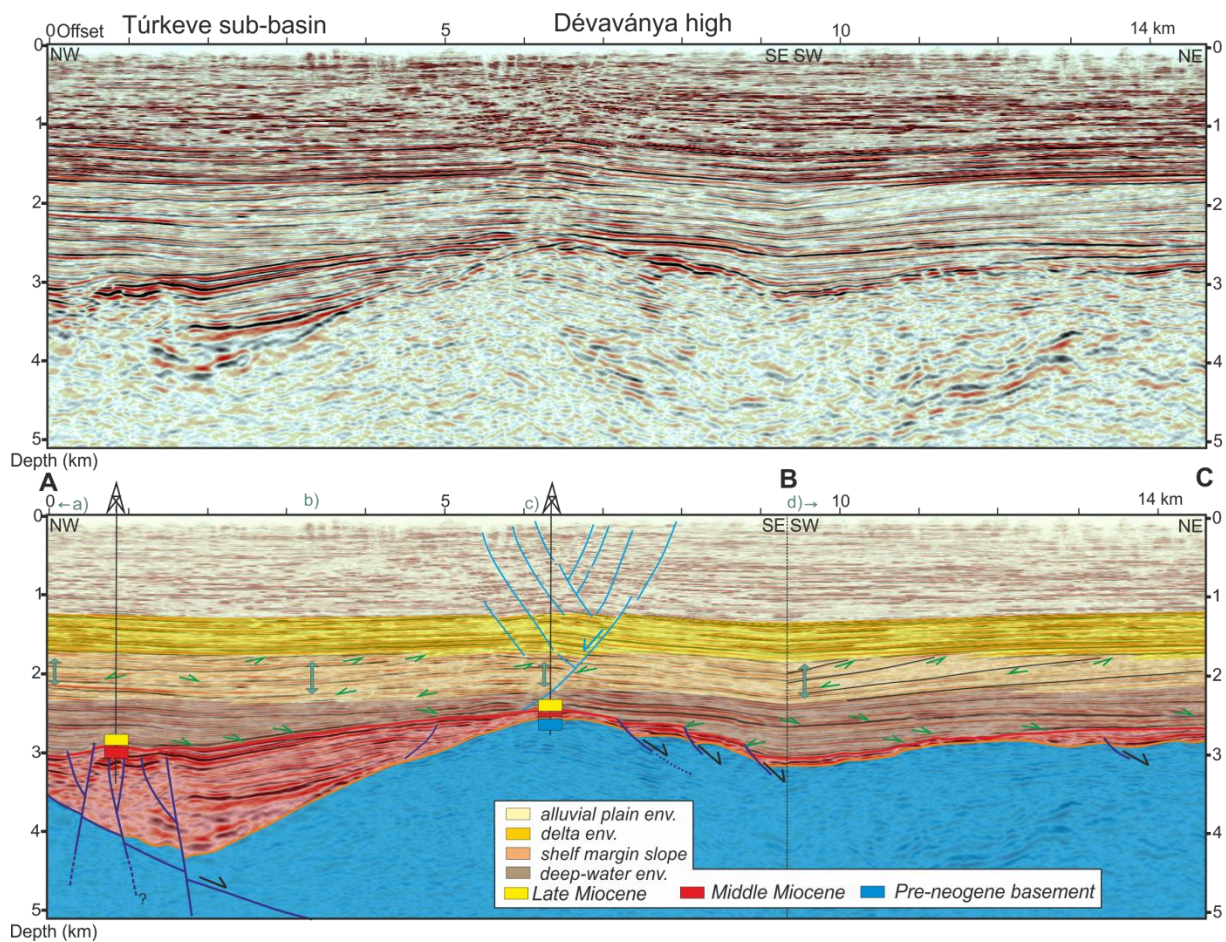


341

342 **Figure 8.** a) Interpreted seismic section located in the NE part of the Pannonian Basin. Location
 343 in Figure 1. The interpretation demonstrates a buried late Middle Miocene (Sarmatian) volcano
 344 beneath the subsequent Late Miocene (Pannonian) sediments. The gentle anticline geometry of
 345 the overlying Pannonian sediments (see arbitrary blue horizon above the volcano highlighted
 346 in the white rectangle) is created by differential compaction, see chapter 5 for details. The red
 347 line is the Middle- Upper Miocene unconformity. Red area indicates further volcanic edifices
 348 and volcano-clastic sediments. Small deltas indicated by numbers are used in Table 1; b) Detail
 349 of the same seismic line showing a prograding delta, observed by downlap reflection
 350 terminations (green arrows).

351 The region of the Nyírség sub-basin in the NE part of the Great Hungarian Plain (Fig. 1)
 352 contains significant amounts of upper Middle Miocene (Sarmatian) rhyolites, rhyodacites and
 353 dacites, domes, lava flows and related tuffs (Pécskay et al., 2006). The analysis of a seismic
 354 line in this sub-basin (Fig. 8) shows such a buried Sarmatian volcanic geometry made up by
 355 extrusive lava flows, sills, and other intrusive complexes, surrounded by high amplitude
 356 reflectors located beneath the base Late Miocene unconformity. The Miocene depocentre is
 357 filled with Middle Miocene volcano-clastic sediments, which is a typical feature observed in

358 many other sub-basins located in a similar tectonic position along the Mid-Hungarian Fault
359 Zone (e.g., Horváth et al., 2015). These Middle Miocene syn-kinematic wedges were deposited
360 against the controlling NE-dipping normal faults (Fig. 8). The fault zone was likely reactivated
361 during earliest Late Miocene times with low reverse and strike-slip offsets creating a flower
362 structure (Fig. 8). Available interpretation infers that the Upper Miocene succession in the
363 Nyírség sub-basin is characterized by geometries of deltaic and alluvial environments with no
364 observed deeper shelf-margin slope clinoform geometries. This suggests that the rate of
365 sedimentation has always kept pace with the local subsidence rate and the absence of inherited
366 paleobathymetries. This is in agreement with observations in one well (Fig. 8) penetrating the
367 entire Upper Miocene succession reporting frequent coal intercalations (Székyné et al., 1985).
368 Laterally to the SW in the analysed seismic lines 10s of meters thick deltaic clinoforms
369 prograding over a shallow shelf are observed within the lowermost Pannonian sediments. The
370 height of these clinoforms increases further SW-ward in the direction of progradation where
371 they become the much larger shelf-margin slope clinoforms observed almost everywhere in the
372 basin. In other words, these clinoforms show the older onset of Late Miocene progradation in
373 the basin that started with low amplitude clinoforms and that gradually increase in height with
374 time indicating an increase of the paleo-water depth. The decompacted height of these initial
375 clinoforms (Fig. 8b, Table 1) is in the order of 70 to 150 meters and were deposited between
376 11.6 - 9 Ma. Their geometries are similar to the transitional slopes interpreted in the western
377 parts of the Pannonian Basin (cf., Sztanó et al., 2015). Note the gentle anticline geometry of the
378 younger Pannonian to Quaternary horizons above the buried volcano. The present-day Tisza
379 river is changing its course significantly around this anticline (Fig. 1).



380
 381 **Figure 9.** Non-interpreted (up) and interpreted (down) seismic depth-converted section from
 382 the central part of the Great Hungarian Plain (location in Figure 1) showing an Early to Middle
 383 Miocene sub-basin and typical Late Miocene seismic facies. Note that the trace of the section
 384 is a composite between a segment parallel with and one perpendicular to the direction of
 385 progradation (BC and AB, respectively). Note the wide segmented fault zone above the
 386 basement high that reflects differential compaction in the sub-basins above the basement high
 387 (see chapter 5 for details). Green arrows are reflection terminations. The four blue double
 388 arrows are locations of paleo-water depth calculations (a-d) within the slope environment.

389 A depth converted seismic section from the Túrkeve sub-basin (Figs. 1, 9) shows a typical
 390 structure for the central part of the Great Hungarian Plain: a half-graben filled with Early to
 391 Middle Miocene syn-extensional sediments is overlain by ~3 km of Late Miocene post-
 392 kinematic deposits. The half-graben is controlled by a large offset SE-dipping low-angle normal

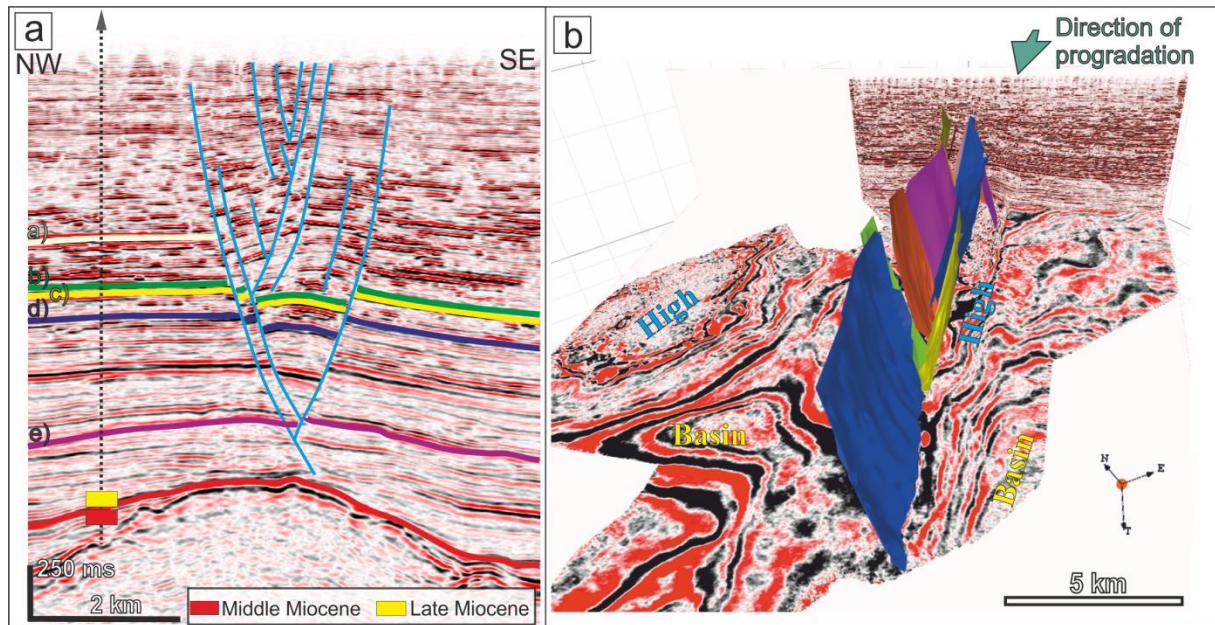
393 fault, which is accompanied by lower offset normal faults. The half-graben is also slightly
394 inverted by a positive flower structure and shows the typical unconformity also observed
395 elsewhere in the Pannonian Basin at the transition between Middle and Late Miocene
396 (Sarmatian to Pannonian). The structural style is otherwise similar to other such Early – Middle
397 Miocene sub-basins (e.g., Kiskunhalas or Vésztő, see also Balazs et al., 2016). The overlying
398 strata show gentle anticline geometry over the Dévaványa basement high (Fig. 9). The typical
399 progradation of shelf-margin slope clinoforms is observed in the overlying Upper Miocene
400 (Pannonian) sediments. The prograding shelf-margin slope reached this sub-basin by
401 prograding SW-wards at about 5.7 Ma (Magyar et al., 2013). The paleo-water depth was
402 calculated in four points along the same spatially correlated timeline (or reflector, Fig. 9, Table
403 1). These calculations show a variable bathymetry at the base of the slope ranging from 475m
404 over the Dévaványa basement high to 630 and 740 m in the region overlying the depocentres.
405 Our calculations thus demonstrate that paleo-bathymetries were controlled by the inherited
406 extensional basin geometries, the base of the slope showing higher values over the various sub-
407 basins when compared with intervening basement highs. This means that the deposition of
408 deep-water pelagic sediments and turbidites was unable to compensate the inherited
409 morphological differences from extensional times before the shelf-margin slope progradation
410 arrived to a proximal position.

411 **5. Compaction-induced folds and faults**

412 Seismic sections from different sub-basins of the Pannonian Basin system show the lateral
413 variation of basement depth created by the variable Miocene crustal thinning and subsequent
414 ongoing differential vertical movements (Figs. 5-9). Late Miocene sediments up to ~6 km thick
415 are affected by different amounts of compaction resulting in gentle fold geometries (Fig. 2) or
416 differential compaction induced faults, such as the fault system above the Dévaványa basement

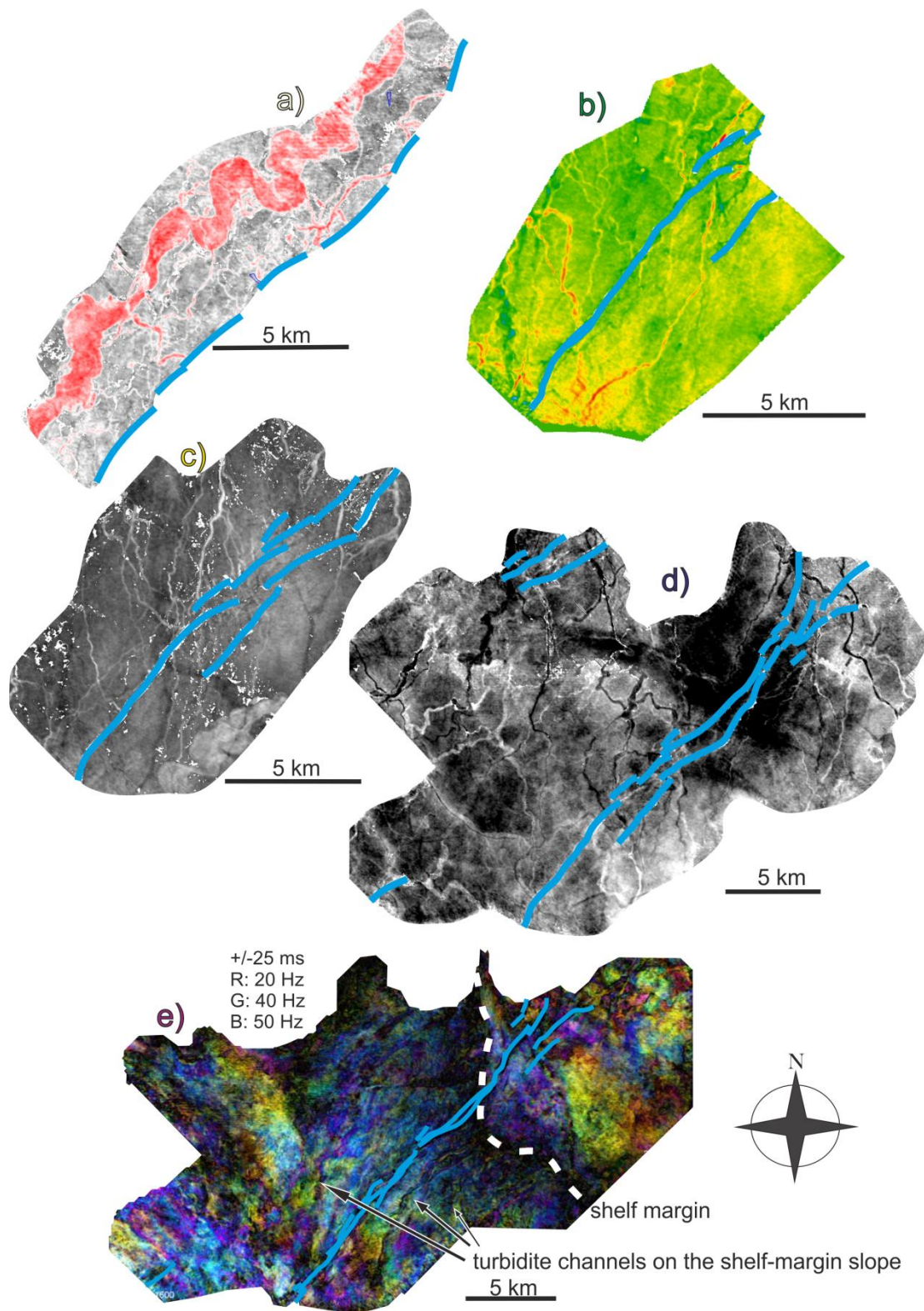
417 high. Compaction induced anticlines are interpreted, for instance, above the buried volcano in
418 the Nyírség sub-basin (Fig. 8) or above the Battonya basement high (Fig. 2).

419



420

421 **Figure 10.** Interpreted seismic data from the central part of the Great Hungarian Plain. Location
422 in Figure 1. a) The segmented Túrkeve Fault zone affecting Late Miocene to Quaternary
423 sediments. Note the increase in offsets upwards in the stratigraphy. The horizons a) to e) were
424 mapped in the seismic cube and are displayed as horizon maps in Figure 11. b) 3D image of the
425 same Túrkeve Fault segments above the basement high, surrounded by deeper basins on either
426 side.



427

428 **Figure 11.** Interpreted seismic horizon maps. Blue lines indicate fault segments cross-cutting
 429 horizons. Figures a) to e) correspond to horizons a-e shown in Figure 10a. (a) Amplitude map
 430 of a horizon from the alluvial plain, illustrating a meandering river and smaller distributaries.

431 (b-d) Amplitude maps of horizons from anastomosing delta plain environments showing
432 meandering and anastomosing channels. (e) Spectral decomposition attribute map of a horizon
433 through the shelf, shelf-margin, slope and deep water environments (see text for further
434 explanations). Note that no channel is displaced horizontally by the fault segments and,
435 therefore, these faults do not show strike-slip displacements.

436 The effects of compaction can be also analysed by the example of the 3-4 km thick
437 sediments overlying the Dévaványa basement high (Figs. 9, 10). The centre of the gentle
438 anticline overlying this basement high (Fig. 9) is cross-cut by a wide normal fault zone
439 truncating the Late Miocene - Quaternary sediments. This fault zone has been previously
440 interpreted either as normal growth fault (e.g., Grow et al., 1994), or a wide strike slip fault
441 zone that is similar to other negative flower structures commonly interpreted in 2D seismic lines
442 in many other areas of the Pannonian Basin (Horváth et al., 2006; Bada et al., 2007).
443 Interestingly, the detailed analysis in this Túrkeve area shows that fault offsets gradually
444 increase upwards from the basement high and furthermore decrease in the uppermost part of
445 the section.

446 The mechanism of formation of this system of normal faults with variable offsets observed
447 above the Dévaványa basement high can be studied in more details on a 3D seismic cube, where
448 individual fault segments and marker horizons cross-cut by faults were mapped (Figs. 10, 11).
449 These faults truncate and offset Pannonian post-rift sediments. The fault with the largest offset
450 dips SE-wards in the southern part of the studied area and changes to a NW-ward dip in the
451 north, where the fault zone is wider (Fig. 10). The maximum throw of the fault is reached within
452 the delta sediments of the Újfalu Formation by ~100 meters. The offset analysis in the 3D cube
453 confirms the observation of the 2D seismic lines of a gradual increase of offset upwards from
454 the oldest Late Miocene deep-water sediments and furthermore a decrease in the uppermost
455 part of the section (Fig. 10). This pattern is a typical attribute of faults related to salt movement

456 and/or differential compaction effects (e.g., Magara, 1978; Williams, 1987; Xu et al., 2015).
457 The absence of salt bodies in our seismic observations and previous studies infers differential
458 compaction effects. A much clearer discrimination from strike-slip deformation is provided by
459 the analysis of horizontal offsets. We have calculated a large number of attribute maps that all
460 show excellent expressions of the faults system and the sedimentology of variable fluvial-
461 alluvial to deltaic environments, from meandering rivers (Fig. 11a) to turbiditic channels on
462 slopes (Fig. 11e). Most of the larger channels are oriented parallel with the normal faults, which
463 is also the strike of the neighbouring older extensional basins and the strike of the basement
464 high. However, smaller channels often cross the various branches of the normal fault system
465 but none of these sedimentary channels indicate any horizontal offset when crossing the various
466 fault branches. As a consequence, the strike-slip kinematics of this zone can be ruled out. We
467 conclude that differential compaction is the primary mechanism creating such structures. This
468 interpretation is also supported by the lack inversion of the underlying basement structure.
469 Initiation of similar extensional faults otherwise can be also associated with the inversion of the
470 underlying basement structures.

471

472 **6. Discussion**

473 **6.1 Controls on water depth variations and progressive infill of Lake Pannon**

474 The main observed mechanism of Late Miocene – Early Pliocene basin infill is the shelf-
475 margin slope progradation. Because the processes controlling the balance between the
476 accommodation space and sediment supply in Lake Pannon have similar orders of amplitude,
477 they create a local fine interplay with aggradational and progradational geometries
478 superimposed on the overall prograding pattern (e.g., Juhász et al., 2007; Sztanó et al., 2013).
479 The controlling factors are coeval thermal subsidence, climatic variations, massive sourcing of

480 sediments from the paleo-Danube and paleo-Tisza rivers, inherited extensional morphology
481 determining bathymetrics and eventual connection at the separating gateways with other basins
482 (e.g., Leever et al., 2010). The relative importance of these forcing factors varied spatially
483 through time.

484 The widespread erosional unconformity at the base of the Late Miocene sediments and the
485 very thin or absent late Middle Miocene (Sarmatian) succession in the centre of the Pannonian
486 Basin (Magyar et al., 1999) suggests an overall shallow water depth or even subaerial
487 environment during the onset of Late Miocene (Pannonian) times. Exceptions are recorded in
488 the deepest Middle Miocene (half-)grabens, such as the Békés basin, and areas near the margins
489 of the Pannonian Basin, like the Danube basin, where Middle Miocene subsidence outpaced
490 sediment supply and, therefore, deep water environments could have continued. This
491 asymmetry of shallow in the centre and deep bathymetry near the margins of the Pannonian
492 Basin was created by the overall variability of the extensional dynamics (Balázs et al., 2016;
493 2017). The base Pannonian unconformity probably also marks the final disconnection of the
494 Lake from the remnant of the Paratethys (Magyar et al., 1999), although the later (Messinian)
495 connectivity of the Pannonian and Dacian and then the Black Sea basins is still under debate
496 (c.f., Magyar and Sztanó, 2008; Leever et al., 2010; Csató et al., 2015; Matenco et al., 2016).

497 After a short break in extension during earliest Pannonian times, rapid subsidence continued
498 in the Pannonian Basin (Horváth et al., 2015; Balázs et al., 2016). This subsidence was locally
499 enhanced by the formation of other Late Miocene half-grabens, mostly concentrated in the E
500 and SE parts of the Pannonian Basin until about 9-8 Ma. Subsidence has created a rapid
501 transgression associated with the deposition of a deep-water facies recorded in most of the
502 Pannonian and Transylvanian basins (e.g., Krézsek et al., 2010). These processes have resulted
503 in highly variable paleo-bathymetries during the evolution of Lake Pannon, as reflected by our
504 calculated heights of the subsequent shelf-margin slope progradation (Fig. 6). In the NW

505 Danube basin, the water depth increased to a minimum of 550 m and the basin was subsequently
506 filled by 9 Ma with ~1.5 km thick deep water sediments. In the NE (e.g., the Nyírség sub-basin)
507 the subsidence and water level rise kept pace with sedimentation, resulting in a small paleo-
508 bathymetrical variability of consistently shallow water prograding – aggrading – retrograding
509 delta and alluvial environments during the entire Late Miocene - Quaternary basin evolution
510 with only a few localized exceptions (Fig. 8). Southwards (near the Nádudvar sub-basin, Fig.
511 6b), the general progradation was interrupted by a major flooding and retrogradation at ~ 7.5
512 Ma. In contrast, the rate of tectonic subsidence was lower in the western parts of the Pannonian
513 Basin resulting in a gradual basin fill by aggradation and progradation. In other words the rates
514 of sediment supply and creation of accommodation space were roughly in balance there. In the
515 centre of the Pannonian Basin (the Danube-Tisza interfluvium, Fig. 1) the subsidence rates were
516 low during the entire evolution and represented a basement high, therefore, the paleo-
517 bathymetry has never reached the few hundreds of meters observed elsewhere (Fig. 6).

518 Because subsidence rates and consequently creation of accommodation continuously
519 decreased with time after the initial Late Miocene transgression, while sediment input remained
520 high or even increased, therefore, the entire Lake Pannon was finally filled by ~4 Ma (Magyar
521 et al., 2013). Smaller scale water level variations are observed by the analysis of the shelf-edge
522 trajectories. Such an isolated lacustrine system is more sensitive to regional climate and
523 therefore lake level variations are interpreted to be climatically driven (Uhrin and Sztanó, 2011;
524 Sztanó et al. 2013) or could be controlled by local subsidence and uplift pulses associated with
525 the late stage inversion of the Pannonian Basin. Our reconstructed paleobathymetries between
526 6.8 Ma and 5 Ma show that the highest water depth values of the lake reached and most probably
527 exceeded values of 1000 m (Table 1, see also Balázs et al., 2015). The asymmetry of the
528 transport direction dominant from the NE and NW during the continuous subsidence has created
529 higher paleo-bathymetries in the SE where progradation was recorded at later times (Fig. 6a).

530 By the same reasoning, these basins contain the largest thicknesses of deep water pelagic
531 sediments and distal turbidites reaching up to 3.5 km (e.g., Sztanó et al., 2013).

532

533 6.2 Shelf-margin morphology and basin evolution

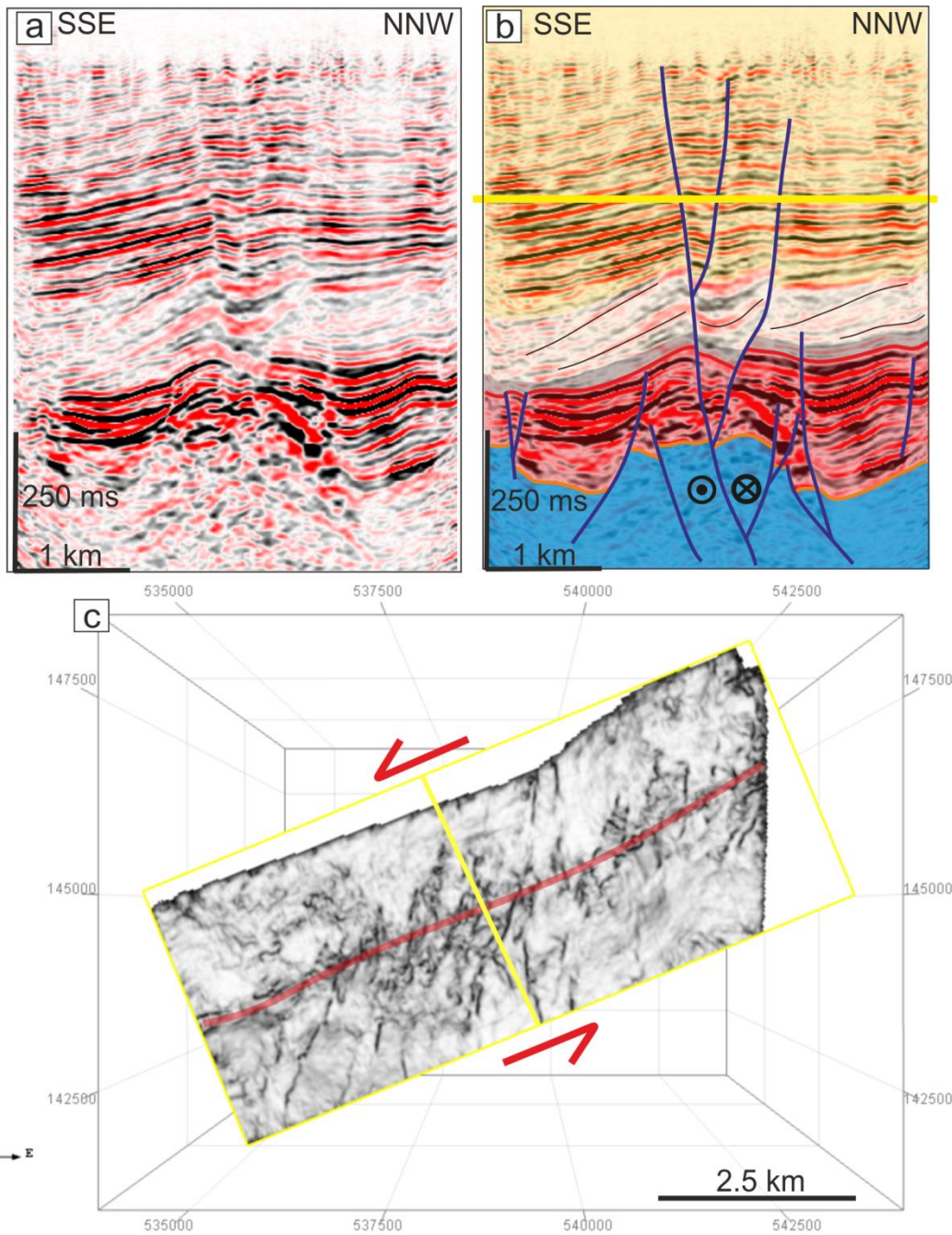
534 Miocene-Pliocene sediments deposited on the slope connecting the shelf with the deep-
535 water basin of Lake Pannon are presently deeply buried in the Pannonian Basin. Our analysis
536 shows that the width of the slope between the shelf-edge to the toe-slope varies between 5 and
537 15 km at decompacted heights between 200 and 1000 m. This results in slope angles between
538 3° and 8°. Such values are similar to dip angles of marine slopes (Porebski and Steel, 2003;
539 Johanessen and Steel 2009; Gong et al., 2016) that are controlled by lithology, grain size
540 distribution or sediment influx from the source area (e.g, Gvirtzman et al., 2014).

541 Our calculations demonstrate that paleo-bathymetries were controlled by the inherited
542 extensional geometries, with higher values (600-700 m at the base of the slope) over the various
543 sub-basins than over the intervening basement highs (400-500 m). This means that the
544 deposition of deep-water pelagic sediments and turbidites was unable to compensate all the
545 inherited morphological differences from extensional times before the shelf-margin slope
546 progradation arrived (see also Törő et al., 2012).

547 Our analysis of the shelf sedimentation (Fig. 7) shows progradation of tens of meters thick
548 deltas (Uhrin and Sztanó, 2011). Their position on the inner or outer shelf is controlled by lake
549 water level variations that typically reach ~100 m during highstands, as observed in marine
550 domains or semi-enclosed seas, such as the Mediterranean (Rabineau et al., 2006) or the Black
551 Sea (Porebski and Steel, 2003; Matenco et al., 2016). Our interpretation of water-level
552 variations infer periods of ascending, descending and stationary shelf-edge trajectories (Fig. 7).
553 Such an analysis does not necessarily take into account the small-scale variations of

554 accommodation on the shelf (cf., Sztanó et al., 2013), but in basins characterized by ongoing
555 tectonic subsidence, such as the Miocene Pannonian Basin, even stationary shelf-edge
556 trajectory indicates periods of climatically-driven water-level fall. Their amplitudes are similar
557 to the rate of basin subsidence. However, in our case their local amplitude is only in the order
558 of tens of meters usually. In contrast with typical passive margin settings, back-arc extension
559 has resulted in highly variable basement morphology, such as deep half-grabens, like for
560 instance the Makó Trough (Fig. 2) or basement highs, like the Transdanubian Range (Fig. 1).
561 These structures also control locally the direction of sediment transport, such as in the Túrkeve
562 sub-area, where the direction of progradation followed the strike of the inherited Middle
563 Miocene sub-basin (Fig., 1, 9) such as in the Sava Trough.

564 The inherited relief, spatially variable subsidence rates and lake water level variations
565 controlled the paleo-bathymetries and created tens of metres high deltaic clinoforms over the
566 shelf and up to 1000 meters high shelf-margin slope clinoforms (c.f., Leroux et al., 2014;
567 Rabineau et al., 2014). Of course, between such end members the balance between the rate of
568 sedimentation and progressively increasing base-level rise could result in the continuous
569 transition from small scale deltas to high shelf-margin slopes (cf. Sztanó et al., 2015). Such
570 transitional slopes are observed in the Nyírség sub-basin (Fig. 8) and its prolongation towards
571 the deep Derecske Trough (Balázs et al., 2016), or in the Danube-Tisza interfluvium. Water depths
572 are in general higher above the former half (grabens) and lower above the separating basement
573 highs.



574

575 **Figure 12.** General geometry of a strike-slip fault zone. Non-interpreted (a) and interpreted (b)
 576 seismic section crossing the Balaton Fault zone, location in Figure 1; c) Coherency cube time
 577 slice highlighting the geometry of synthetic Riedel faults and demonstrating the sinistral strike-
 578 slip offset of this fault zone (see also Várkonyi et al., 2013 and Visnovitz et al., 2015).

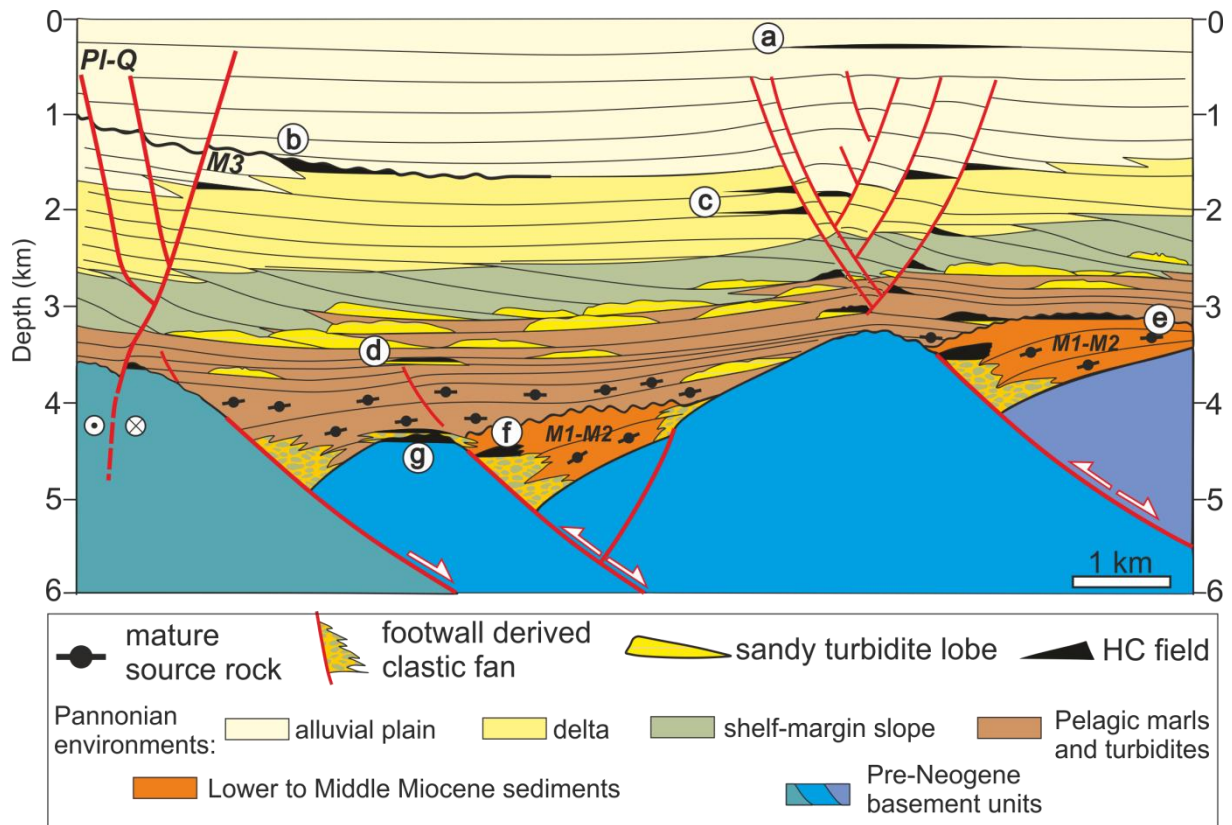
579 The syn-rift extension and half-graben formation in the Pannonian Basin ultimately
 580 ceased at 8-9 Ma (e.g., Matenco and Radivojevic, 2012; Balázs et al., 2017). The subsequent

581 evolution was controlled by post-rift thermal cooling and the basin-wide inversion during the
582 Adriatic indentation creating differential vertical movements (Fig. 1; Sacchi et al., 1999; Bada
583 et al., 2007). Such inverted structures are well documented from earliest late Miocene times in
584 the western part of the Pannonian Basin (Fodor et al., 2005; Uhrin et al., 2009), at 6-8 Ma along
585 the Mid-Hungarian Fault zone (Fig. 6d, see also Juhász et al., 2013). Our results show that
586 effects of basin inversion should be taken into account significantly during the calculation of
587 the paleo-bathymetries in the entire basin. The observed contraction reached a peak at the
588 transition between Miocene and Pliocene times, caused likely by the northward drift and CCW
589 rotation of the Adriatic microplate (Pinter et al., 2005). This peak contraction is the main
590 mechanism creating the widespread unconformity observed at the transition between the
591 Miocene and Pliocene in the Pannonian Basin (e.g., Fig. 7), being replaced laterally by a
592 correlative conformity in deeper sub-basins (Magyar and Sztanó, 2008). Our observations
593 confirm that the Late Miocene to Recent evolution of the Pannonian Basin and associated
594 subsidence/uplift pattern is mainly controlled by basin scale flexural effects superimposed on
595 post-rift thermal sagging (Horváth and Cloetingh, 1996; Dombrádi et al., 2010; Jarosinski et
596 al., 2011).

597 Previous interpretations assumed that the inversion was also associated with the
598 (re)activation of strike slip zones along former structures (Fig. 1; Horváth et al., 2006, Bada et
599 al., 2007; Visnovitz et al., 2015). Strike-slip kinematics are certainly significant in many parts
600 of the Pannonian Basin, demonstrated by the observation of offsets and Riedel shears in 2D or
601 3D seismics (e.g., Fig. 12, see also Várkonyi et al., 2013). However, our study demonstrates for
602 the first time that compaction effects creating fault systems such as the one quantified above
603 the Dévaványa basement high are certainly significant in the sediments of the Pannonian Basin.
604 The effects should be similar elsewhere: faults with variable offsets, increasing and

605 subsequently decreasing towards the surface, reaching a maximum in the order of 150 m (Figs.
 606 9, 13).

607



609 **Figure 13.** Conceptual model of the Neogene basin fill in the Great Hungarian Plain that takes
 610 into account the morphology of the bed of Lake Pannon, including inherited extensional
 611 structures and further effects, such as differential compaction over basement highs and
 612 neotectonic strike-slip fault zones (modified after Tari and Horváth, 2006). Figure also shows
 613 the main hydrocarbon play types of the basin: a) Biogenic and thermogenic fields in drape-folds
 614 above basement highs; b) stratigraphic traps in delta sandstones or connected to unconformities;
 615 c) delta or deep-water turbiditic sandstones affected by compaction induced normal faults; d)
 616 stratigraphic or structural traps in deep-water turbiditic sandstones. e) Sandstones and
 617 conglomerates at the unconformity of inverted Early-, Middle- Miocene basins; f) footwall-
 618 derived fans along the boundary faults of half-grabens; g) basal conglomerates deposited onto

619 the basement or the fractured Neogene-basement itself. Differential compaction induced faults
620 at the periphery of half grabens may provide migration pathways.

621 **7. Conclusions**

622 Our interpretation of 2D and 3D seismic data correlated with well logs from the Late-
623 Miocene to Quaternary sedimentary succession filling the Pannonian Basin shows a transition
624 from an initially underfilled to a finally overfilled large lacustrine basin. Spatial and temporal
625 variations of the external and internal forcing factors resulted in lateral changes of prograding
626 – aggrading – retrograding shelf-margin slope geometries and paleo-water depths. Using
627 decompacted thicknesses of the prograding shelf-margin slope clinoforms, our calculations
628 indicate the variation of water depth values from ~75 m up to ~1 km. Highest water depth values
629 characterized the SE part of the basin as a consequence of higher subsidence rates and more
630 distal position from the source areas. The shelf had paleo-bathymetries of up to 75 m with a
631 high order variability controlled by climate. Both water depth and sedimentary transport routes
632 were primarily determined by inherited and/or active local tectonics; they controlled Late
633 Miocene shelf-margin progradation directions as well as Recent fluvial transport routes.

634 Latest Miocene to Recent tectonic topography appears to be basin scale folding process.
635 Areas of uplift were subject to denudation and the eroded material continuously overfilled the
636 generated accommodation space. Sediments up to ~6 km have been affected by this still
637 ongoing differential vertical movement and compaction creating gentle fold geometries and
638 differential compaction induced fault offsets, playing a major role in hydrocarbon migration
639 and trapping (Fig. 13). Geometries of such non-tectonic faults above basement highs can be
640 clearly distinguished from extensional or strike-slip fault geometries by the calculation and
641 analysis of 3D seismic attributes.

642 **Acknowledgements**

643 This study was financed by the Netherlands Centre for Integrated Solid Earth Science
644 (ISES) and Eötvös Loránd University, Budapest in a collaborative study of the Pannonian
645 Basin. MOL Plc. and Hungarian Horizon Energy Ltd. are acknowledged for providing seismic
646 and well data. The first and sixth authors (AB & FH) are grateful to the academic support of
647 the Hungarian Science Foundation (OTKA K-109255). OTKA no. 113013 and NKFIH no.
648 116618 funds are also acknowledged. This is MTA-MTM-ELTE Paleo contribution No. X.
649 Seismic interpretation was carried out by the IHS Kingdom and dGB OpendTect software,
650 which we could use as participants of the IHS and dGB University Software Grant Programs.
651 Didier Granjeon, László Fodor and Gábor Bada are thanked for stimulating discussions. We
652 thank the reviewers Marina Rabineau, Csaba Krézsek and Gábor Tari for their constructive
653 remarks that have improved the manuscript.

654

655 **References**

656

657 Angevine, C.L., Heller, P.L., Paola, C., 1990. Quantitative sedimentary basin modelling. AAPG
658 Course Note Series 32, 133 pp.

659 Bada, G., Horváth, F., Dövényi, P., Szafián, P., Windhoffer, G., Cloetingh, S., 2007. Present-
660 day stress field and tectonic inversion in the Pannonian basin. *Global and Planetary*
661 *Change* 58, 165-180.

662 Balázs, A., Tókécs, L., Magyar, I., 2015. 3D analysis of compaction related tectonic and
663 stratigraphic features of the Late Miocene succession from the Pannonian Basin.
664 Abstract Book of 31st IAS Meeting of Sedimentology 1–52.

665 Balázs, A., Matenco, L., Magyar, I., Horváth, F., Cloetingh, S., 2016. The link between
666 tectonics and sedimentation in back-arc basins: new genetic constraints from the

667 analysis of the Pannonian Basin. *Tectonics* 35, 1526–1559, doi:
668 10.1002/2015TC004109

669 Balázs, A., Burov, E., Matenco, L., Vogt, K., Francois, T., Cloetingh, S., 2017. Symmetry
670 during the syn- and post-rift evolution of extensional back-arc basins: the role of
671 inherited orogenic structures. *Earth and Planetary Science Letters* 462, 86-98.

672 Báldi, T., 1986. Mid-Tertiary stratigraphy and Paleogeographic evolution of Hungary.
673 Budapest, Akadémiai Kiadó 201.

674 Bérczi, I., Phillips, R.L., 1985. Process and depositional environments within Neogene deltaic–
675 lacustrine sediments, Pannonian Basin, Southeast Hungary. *Geophysical Transactions*
676 31, 55–74.

677 Carroll, A. R., Bohacs, K. M., 1999. Stratigraphic classification of ancient lakes: balancing
678 tectonic and climatic controls. *Geology* 27, 99-102.

679 Cartwright, J., Huuse, M., 2005. 3D seismic technology: the geological 'Hubble'. *Basin*
680 *research* 17, 1-20.

681 Chopra, S., Marfurt, K. J., 2005. Seismic attributes. – A historical perspective. *Geophysics* 70,
682 3.

683 Cloetingh, S., Van Wees, J. D., Ziegler, P., Lenkey, L., Beekman, F., Tesauro, M., Förster, A.,
684 Norden, B., Kaban, M., Hardebol, N., Bonté, D., Genter, A., Guillou-Frottier, L.,
685 Voorde, M. T., Sokoutis, D., Willingshofer, E., Cornu, T., and Worum, G., 2010.
686 Lithosphere tectonics and thermo-mechanical properties: An integrated modelling
687 approach for Enhanced Geothermal Systems exploration in Europe. *Earth-Sci. Rev.*
688 102, 159–206, 2010.

689 Csató, I., Tóth, S., Catuneanu, O., Granjeon, D., 2015. A sequence stratigraphic model for the
690 Upper Miocene–Pliocene basin fill of the Pannonian Basin, eastern Hungary. *Marine*
691 *and Petroleum Geology* 66, 117-134. doi: 10.1016/j.marpetgeo.2015.02.010

692 Csontos, L., Nagymarosy, A., 1998. The Mid-Hungarian line: a zone of repeated tectonic
693 inversions. *Tectonophysics* 29, 51-71.

694 De Leeuw, A., Mandic, O., Krijgsman, W., Kuiper, K., Hrvatović, H., 2012. Paleomagnetic and
695 geochronologic constraints on the geodynamic evolution of the Central Dinarides.
696 *Tectonophysics* 530—531, 286-298.

697 Dombrádi, E., Sokoutis, D., Bada, G., Cloetingh, S., Horváth, F., 2010. Modelling recent
698 deformation of the Pannonian lithosphere: Lithospheric folding and tectonic
699 topography. *Tectonophysics* 484, 103-118.

700 Dövényi, P., 1994. Geofizikai vizsgálatok a Pannon-medence litoszféafejlődésének
701 megértéséhez. MTA thesis, Hungarian Academy of Sciences, Budapest, 127 p. (in
702 Hungarian).

703 Faccenna, C., Becker, T. W., Auer, L., Billi, A., Boschi, L., Brun, J. P., Capitanio, F. A.,
704 Funiciello, F., Horváth, F., Jolivet, L., 2014. Mantle dynamics in the Mediterranean. *Rev.*
705 *Geophys.* 52, 283–332, doi:10.1002/2013RG000444.

706 Fodor, L., Bada, G., Csillag, G., Horvath, E., Ruzs-kiczay-Rudiger, Z., Palotas, K., Sikhegyi, F.,
707 Timar, G., Cloetingh, S., 2005. An outline of neotectonic structures and
708 morphotectonics of the western and central Pannonian Basin. *Tectonophysics* 410, 15-
709 41.

710 Fongngern, R., Olariu, C., Steel, R. J., Krézsek, Cs., 2015. Cliniform growth in a Miocene,
711 Para-tethyan deep lake basin: Thin topsets, irregular foresets and thick bottomsets.
712 *Basin Research* 28, 770–795.

713 Garcia-Castellanos, D., Verges, J., Gaspar-Escribano, J., Cloetingh, S., 2003. Interplay between
714 tectonics, climate, and fluvial transport during the Cenozoic evolution of the Ebro
715 Basin (NE Iberia). *J. Geophys. Res.* 108, 2347.

716 Gong, C., Steel, R., Wang, Y., Lin, C., Olariu, C., 2016. Shelf-margin architecture variability
717 and its role in sediment-budget partitioning into deep-water areas. *Earth-Science*
718 *Reviews* 154, 72-101.

719 Grow, J.A., Mattick, R.E., Bérczi-Makk, A., Péró, Cs., Hajdú, D., Pogácsás, Gy., Várnai, P.,
720 Varga, E., 1994. Structure of the Békés Basin Inferred from Seismic Reflection, Well
721 and Gravity Data. In: Teleki, et al. (Eds.), *Basin Analysis in Petroleum Exploration*.
722 Kluwer Academic Publishers, Dordrecht, 1–37.

723 Gvirtzman, Z., Csató, I., Granjeon, D., 2014. Constraining sediment transport to deep marine
724 basins through submarine channels: the Levant margin in the Late Cenozoic. *Mar.*
725 *Geol.* 347, 12–26.

726 Helland-Hansen, W., Hampson, G.J., 2009. Trajectory analysis: concepts and applications.
727 *Basin Research* 21, 454–483.

728 Henriksen, S., Helland-Hansen, W., Bullimore, S., 2011. Relationship between shelfedge
729 trajectories and sediment dispersal along depositional dip and strike: a different
730 approach to sequence stratigraphy. *Basin Research* 23, 3–21.

731 Horváth, F., Bada, G., Windhoffer, G., Csontos, L., Dombrádi, E., Dövényi, P., Fodor, L.,
732 Grenczy, Gy, Síkhegyi, F., Szafián, P., Székely, B., Timár, G., Tóth, L., Tóth, T.,
733 2006. A Pannon-medence jelenkori geodinamikájának atlasza: Euro-konform
734 térképsorozat és magyarázó. *Magyar Geofizika* 47, 133–137 (in Hungarian, with
735 English abstract).

736 Horváth, F., Cloetingh, S., 1996. Stress-induced late-stage subsidence anomalies in the
737 Pannonian basin. *Tectonophysics* 266, 287-300.

738 Horváth, F., Musitz, B., Balázs, A., Végh, A., Uhrin, A., Nádor, A., Koroknai, B., Pap, N.,
739 Tóth, T., Wórum, G., 2015. Evolution of the Pannonian basin and its geothermal
740 resources. *Geothermics* 53, 328-352.

741 Jarosinski, M., Beekman, F., Matenco, L., Cloetingh, S., 2011. Mechanics of basin inversion:
742 Finite element modelling of the Pannonian Basin System. *Tectonophysics* 502, 121-
743 145.

744 Johannessen, E.P., Steel, R.J., 2005. Shelf-margin clinoforms and prediction of deepwater
745 sands. *Basin Research* 17, 521–550.

746 Juhász Gy., Pogácsás Gy., Magyar I., Hatalyák P., 2013. The Alpar canyon system in the
747 Pannonian Basin, Hungary – its morphology, infill and development. *Global Planet.*
748 *Change* 103, 174–192.

749 Juhász, Gy, Pogácsás, Gy, Magyar, I., Vakarcs, G., 2007. Tectonic versus climatic control on
750 the evolution of fluvio–deltaic systems in a lake basin, Eastern Pannonian Basin.
751 *Sedimentary Geology* 202, 72–95.

752 Juhász, Gy., 1991. Lithostratigraphical and sedimentological framework of the Pannonian (s.l.)
753 sedimentary sequence in the Hungarian Plain (Alföld), Eastern Hungary. *Acta*
754 *Geologica Hungarica* 34, 53–72.

755 Katz, B.J., 1990. Lacustrine basin exploration – Case Studies and Modern Analogues. American
756 Association of Petroleum Geologists Memoir 50, 340 pp. AAPG, Tulsa.

757 Krézsek, C., Filipescu, S., Silye, L., Matenco, L., Doust, H., 2010. Miocene facies associations
758 and sedimentary evolution of the Southern Transylvanian Basin (Romania):
759 Implications for hydrocarbon exploration. *Marine and Petroleum Geology* 27, 191-
760 214.

761 Kovác, M., Andreyeva-Grigorovich, A., Bajraktarevic, Z., Brzobohatý, R., Filipescu, S., Fodor,
762 L., Harzhauser, M., Nagymarosy, A., Oszczytko, N., Pavelic, D., 2007. Badenian
763 evolution of the Central Paratethys Sea: paleogeography, climate and eustatic sea-level
764 changes. *Geologica Carpathica* 58, 579-606.

- 765 Leever, K.A., Matenco, L., Rabagia, T., Cloetingh, S., Krijgsman, W., Stoica, M., 2010.
766 Messinian sea level fall in the Dacic Basin (Eastern Paratethys): palaeogeographical
767 implications from seismic sequence stratigraphy. *Terra Nova* 22, 12–17.
- 768 Leever, K.A., Matenco, L., Garcia-Castellanos, D., Cloetingh, S.A.P.L., 2011. The evolution
769 of the Danube gateway between Central and Eastern Paratethys (SE Europe): insight
770 from numerical modelling of the causes and effects of connectivity between basins and
771 its expression in the sedimentary record. *Tectonophysics* 502, 175–195.
- 772 Leroux, E., Rabineau, M., Aslanian, D., Granjeon, D., Droz, L., Gorini, C., 2014. Stratigraphic
773 simulations of the shelf of the Gulf of Lions: testing subsidence rates and sea-level
774 curves during the Pliocene and Quaternary. *Terra Nova* 26, 230-238.
- 775 Magara, K., 1978. *Compaction and fluid migration*. Elsevier, 349 pp. Amsterdam/New York.
- 776 Magyar, I., Radivojevic, D., Sztanó, O., Synak, R., Ujszászi, K., Pócsik, M., 2013. Progradation
777 of the paleo-Danube shelf margin across the Pannonian Basin during the Late Miocene
778 and Early Pliocene. *Global and Planetary Change* 103, 168–173.
- 779 Magyar, I., Fogarasi, A., Vakarcs, G., Bukó, L., Tari, G.C., 2006. The largest hydrocarbon field
780 discovered to date in Hungary: Algyő. In: Golonka, J., Picha, F.J. (Eds.), *The Carpathians
781 and their foreland: geology and hydrocarbon resources*. AAPG Memoir 84, pp. 619–632.
782 AAPG, Tulsa.
- 783 Magyar, I., Geary, D. H., Müller, P., 1999. Paleogeographic evolution of the Late Miocene
784 Lake Pannon in Central Europe. *Palaeogeogr. Palaeoclimatol. Palaeoecol.* 147, 151-
785 167.
- 786 Magyar, I., Sztanó, O., 2008. Is there a Messinian unconformity in the Central Paratethys?
787 *Stratigraphy* 5, 245-255.
- 788 Martins-Neto, M.A., Catuneanu, O., 2010. Rift Sequence Stratigraphy. *Marine and Petroleum
789 Geology* 27, 247-253.

790 Márton, E., Fodor, L., 2003. Tertiary paleomagnetic results and structural analysis from the
791 Transdanubian Range (Hungary): rotational disintegration of the Alcapa unit.
792 *Tectonophysics* 363, 201-224.

793 Matenco, L., Munteanu, I., ter Borgh, M., Stanica, A., Tilita, M., Lericolais, G., Dinu, C., Oaie,
794 G., 2016. The interplay between tectonics, sediment dynamics and gateways evolution
795 in the Danube system from the Pannonian Basin to the western Black Sea. *Science of*
796 *The Total Environment* 543, 807-827. doi: 10.1016/j.scitotenv.2015.10.081

797 Matenco, L., Radivojević, D., 2012. On the formation and evolution of the Pannonian Basin:
798 Constraints derived from the structure of the junction area between the Carpathians
799 and Dinarides. *Tectonics* 31(6), TC6007.

800 Mészáros, F. Zilahi-Sebess, L., 2001. Compaction of sediments with great thickness in the
801 Pannonian Basin. *Geophysical Transactions* 44, 21-48.

802 Nagymarosy, A., Hámor, G., 2012. Genesis and evolution of the Pannonian Basin, in *Geology*
803 *of Hungary, Regional Geology Reviews*, edited by J. Haas, pp. 149-200, Springer.

804 Nagymarosy, A., Müller, P., 1988. Some aspects of the Neogene biostratigraphy in the
805 Pannonian Basin. in: *The Pannonian Basin, a study in basin evolution*, edited by L. H.
806 Royden and F. Horvath, AAPG Memoir 45, pp. 58-68. AAPG, Tulsa.

807 Partyka, G., Gridley, J., Lopez, J., 1999. Interpretational applications of spectral decomposition
808 in reservoir characterization. *The Leading Edge* 18, 353–360.

809 Pécskay, Z., Lexa, J., Szakács, A., Seghedi, I., Balogh, K., Konecny, V., Zelenka, T., Kovacs,
810 M., Póka, T., Fülöp, A., Márton, E., Panatiotu, C., Cvetkovic, V., 2006. Geochronol-
811 ogy of Neogene magmatism in the Carpathian arc and intra-Carpathian area. *Geol.*
812 *Carpathica* 57, 511–530.

- 813 Pinter, N., Greenczy, Gy., Weber, J., Stein, S., Medak D., (Eds.), 2005. The Adria Microplate:
814 GPS Geodesy, Tectonics and Hazards (Nato Science Series: IV: Earth and
815 Environmental Sciences), 413 pp., Springer.
- 816 Pogácsás, Gy., Lakatos, L., Révész, I., Ujszászi, K., Vakarcs, G., Várkonyi, L., Várnai, P., 1988.
817 Seismic facies, electro facies and Neogene sequence chronology of the Pannonian
818 Basin. *Acta Geologica Hungarica* 31, 175–207.
- 819 Porebski, S.J., Steel, R.J., 2003. Shelf-margin deltas: their stratigraphic significance and
820 relation to deepwater sands. *Earth-Science Reviews* 62, 283–326.
- 821 Posamentier, H.W., Walker, R.G., 2006. Deep water turbidites and turbiditic fans, in:
822 Posamentier, H.W., Walker, R.G. (Eds.), *Facies models revisited*. Society for
823 *Sedimentary Geology* pp. 339-527.
- 824 Rabineau, M., Berné, S., Olivet, J.-L., Aslanian, D., Guillocheau, F., Joseph, P., 2006. Paleo
825 sea levels reconsidered from direct observation of paleoshoreline position during
826 Glacial Maxima (for the last 500,000 yr). *Earth Planet. Sci. Lett.* 252, 119–137.
- 827 Rabineau, M., Leroux, E., Aslanian, D., Bache, F., Gorini, C., Moulin, M., Molliex, S., Droz,
828 L., Reis, A.D., Rubino, J.-L., Guillocheau, F., Olivet, J.-L., 2014. Quantifying
829 subsidence and isostatic readjustment using sedimentary pale-omarkers, example from
830 the Gulf of Lions. *Earth Planet. Sci.Lett.* 388, 1–14.
- 831 Rögl, F., Daxner-Höck, G., 1996. Late Miocene Paratethys Correlations. In: Bernor R.L.,
832 Fahlbusch, V., Mittmann, H-W. (eds.), *The evolution of western Eurasian Neogene*
833 *mammal faunas*. Columbia University Press, New York, 47-55
- 834 Royden, L. H., Horváth, F. (eds) 1988. *The Pannonian Basin: a Case Study in Basin Evolution*.
835 American Association of Petroleum Geologists Memoir 45. 394 p. AAPG, Tulsa.
- 836 Sacchi, M., Horváth, F., Magyar, O., 1999. Role of unconformity-bounded units in the
837 stratigraphy of the continental record: A case study from the late Miocene of the

838 western Pannonian Basin, Hungary, in *The Mediterranean Basins: Extension Within*
839 *the Alpine Orogen*, edited by B. Durand et al., *Geol. Soc. Spec. Publ.*, 156, 357–390.

840 Saftic, B., Velic, J., Sztanó, O., Juhász, Gy., Ivkovic, Z., 2003. Tertiary subsurface facies,
841 source rocks and hydrocarbon reservoirs in the SW part of the Pannonian Basin
842 (Northern Croatia and South-Western Hungary). *Geologica Croatica* 56, 101–122.

843 Schmid, S.M., Bernoulli, D., Fugenschuh, B., Matenco, L., Schefer, S., Schuster, R., Tischler,
844 M., Ustaszewski, K., 2008. The Alpine–Carpathian–Dinaridic orogenic system:
845 correlation and evolution of tectonic units. *Swiss J Geosci.* 101, 139–183.

846 Steckler, M.S., Mountain, G.S., Miller, K.G., Christie-Blick, N., 1999. Reconstruction of
847 Tertiary progradation and clinoform development on the New Jersey passive margin
848 by 2-D backstripping. *Marine Geology* 154, 399-420.

849 Szalay, Á., 1982. A rekonstrukciós szemléletű földtani kutatás lehetőségei a
850 szénhidrogénperspektívák előrejelzésében. Kandidátusi dolgozat, Hungarian
851 Academy of Sciences, Budapest, 146 p. (in Hungarian).

852 Szalay, Á., Szentgyörgyi, K., 1988. A Method for Lithogenetic Subdivision of Pannonian (s. l.)
853 Sedimentary Rocks. in: *The Pannonian Basin, a study in basin evolution*, edited by L.
854 H. Royden and F. Horváth, pp. 89-96. AAPG Mem., AAPG, Tulsa.

855 Székyné Fux, V., Pap, S., Barta, I., 1985. A nyírségi Nagyecséd-I. és Komoró-I. fúrások földtani
856 eredményei. *Földtani Közlöny* 115, 63-77 (in Hungarian, with English abstract).

857 Sztanó, O., Magyar, I., Horváth, F., 2007. Changes of water depth in the Late Miocene Lake
858 Pannon revisited: the end of an old legend. *Geophysical Research Abstracts* 9,
859 38897836.

860 Sztanó, O., Sebe, K., Csillag, G., Magyar, I., 2015. Turbidites as indicators of paleotopography,
861 Upper Miocene Lake Pannon, Western Mecsek Mountains (Hungary). *Geologica*
862 *Carpathica* 66, 331-344.

863 Sztanó, O., Szafián P., Magyar, I., Horányi, A., Bada, G., Hughes, D.W., Hoyer, D.L., Wallis,
864 R. J., 2013. Aggradation and progradation controlled clinothems and deep-water sand
865 delivery model in the Neogene Lake Pannon, Makó Trough, Pannonian Basin, SE
866 Hungary. *Global and Planetary Change* 103, 149–167.

867 Tari, G.C., Horváth, F., 2006. Alpine evolution and hydrocarbon geology of the Pannonian
868 Basin: An overview. In: Golonka, J., Picha, F.J. (Eds.), *The Carpathians and their
869 foreland: Geology and hydrocarbon resources*. AAPG Memoir 84, 605–618.

870 ter Borgh, M., Radivojević, D., Matenco, L., 2015. Constraining forcing factors and relative
871 sea-level fluctuations in semi-enclosed basins: the Late Neogene demise of Lake
872 Pannon. *Basin Research* 27, 681-695. doi: 10.1111/bre.12094.

873 ter Borgh, M., Vasiliev, I., Stoica, M., Knežević, S., Matenco, L., Krijgsman, W., Rundić, L.,
874 Cloetingh, S., 2013. The isolation of the Pannonian basin (Central Paratethys): New
875 constraints from magnetostratigraphy and biostratigraphy. *Global and Planetary
876 Change* 103, 99-118.

877 Törő, B., Sztanó, O., Fodor L., 2012. Aljzatmorfológia és aktív deformáció által befolyásolt
878 pannó-niai lejtőépülés Észak-Somogyban. *Földtani Közlöny* 142, 445-468 (in
879 Hungarian, with English abstract).

880 Uhrin, A., Magyar, I., Sztanó, O., 2009. Effect of basement deformation on the Pannonian
881 sedimentation of the Zala Basin, SW Hungary. *Földtani Közlöny* 139, 273-282 (in
882 Hungarian, with English abstract).

883 Uhrin, A., Sztanó, O., 2011. Water-level changes and their effect on deepwater sand
884 accumulation in a lacustrine system: a case study from the Late Miocene of western
885 Pannonian Basin, Hungary. *International Journal of Earth Sciences* 101, 1427-1440.
886 dx.doi.org/10.1007/s00531-011-0741-4.

- 887 Ustaszewski, K., Herak, M., Tomljenović, B., Herak, D., Matej, S., 2014. Neotectonics of the
888 Dinarides-Pannonian Basin transition and possible earthquake sources in the Banja
889 Luka epicentral area. *J. Geodyn.* 82, 52–68.
- 890 Ustaszewski, K., Kounov, A., Schmid, S.M., Schaltegger, U., Krenn, E., Frank, W.,
891 Fügenschuh, B., 2010. Evolution of the Adria-Europe plate boundary in the northern
892 Dinarides: From continent-continent collision to back-arc extension. *Tectonics* 29,
893 TC6017, doi: 6010.1029/2010tc002668.
- 894 Vakares, G., Vail, P. R., Tari, G., Pogácsás, Gy., Mattick, R. E., Szabó, A., 1994. Third-order
895 Middle Miocene-Early Pliocene depositional sequences in the prograding delta
896 complex of the Pannonian Basin. *Tectonophysics* 240, 81-106.
- 897 Várkonyi, A., Törő, B, Sztanó, O, Fodor, L., 2013. Late Cenozoic deformation and tectonically
898 controlled sedimentation near the Balaton zone (central Pannonian basin, Hungary).
899 Occasional Papers of the Geological and Geophysical Institute of Hungary 72–73.
900 ISSN 2064-0293, ISBN 978-963-671-294-5
- 901 Visnovitz, F., Horváth, F., Fekete, N., Spiess, V., 2015. Strike-slip tectonics in the Pannonian
902 Basin based on seismic surveys at Lake Balaton. *Int. J. Earth Sci.* 104, 2273-2285.
- 903 Williams, S.R.J., 1987. Faulting in abyssal-plain sediments, Great Meteor East, Madeira
904 Abyssal Plain. *Geol. Soc. Lond. Spec. Publ.* 31, 87–104.
- 905 Xie, X., Heller, P.L., 2009. Plate tectonics and basin subsidence history. *GSA Bulletin* 121, 55–
906 64. doi:10.1130/B26398.1.
- 907 Xu, S., Hao, F., Xu, C., Wang, Y., Zou, H., Gong, C., 2015. Differential compaction faults and
908 their implications for fluid expulsion in the northern Bozhong Sub-basin, Bohai Bay
909 Basin, China. *Marine and Petroleum Geology* 63, 1–16.

910